

Université de Montréal

**Reactive Hyperemia as endothelial function determinant using
plethysmography methods**

By
Nina Olamaei

In the
**Biomedical Engineering Institute
Faculty of Medicine**

Presented to the Faculty of graduate studies
in partial fulfillment of the requirements for the degree of Master of applied science
in biomedical engineering at Montreal University
Montreal, Quebec, Canada

January 2009

© Nina Olamaei, 2009

Université de Montréal
Faculty of graduate studies

This thesis entitled:
Reactive Hyperemia as endothelial function determinant using plethysmography methods

Presented by:
Nina Olamaei

was evaluated by a jury made up of the following people:

Hervé GAGNON
President-reporter

François HAREL
Supervisor

Anique DUCHARME
Member of jury

Abstract

Atherosclerotic diseases are mainly caused by coronary and peripheral blood vessel disorders. Endothelial dysfunction represents an early phase in these diseases, when patients are generally asymptomatic.

We developed a technique, based on near infrared spectroscopy (NIRS), for measurement of arterial blood flow variations in limbs during reactive hyperemia. The technique allows the study of the level of vascular impairment and probably quantifying the level of endothelial dysfunction at peripheral arteries.

The experiment was performed on two cohorts of 13 and 15 patients and was compared to strain gauge plethysmography (SGP) which is considered as gold standard.

Afterward, we characterized endothelial reaction during reactive hyperemia through blood flow variations by modeling the hyperemic curve. Preliminary studies have shown that the hyperemic response generally adopts a bimodal form. The first peak was attributed to myogenic reaction that is endothelial independent and the second one to local endothelial cells reaction. The quantification of the two hyperemic response components makes it possible to calculate an index of 'health' for local endothelial cells, named *ηfactor*.

The results showed a strong correlation ($r = 0.91$) of blood flow measurements between the developed method and the gold standard. We concluded that NIRS is a precise technique for non-invasive measurement of blood flow. Moreover, we found a high repeatability (ICC = 0.9313) of the *ηfactor* in repeated measurements indicating its robustness. Nonetheless, more studies are required to validate the diagnosis value of the defined factor.

Key words: reactive hyperemia, myogenic response, endothelial dependent vasodilatation, nitric oxide, atherosclerosis, near infrared spectroscopy (NIRS)

Résumé

L'atteinte de la fonction endothéliale représente une phase précoce de l'athérosclérose, un stade où les patients sont généralement asymptomatiques. Il existe donc un intérêt certain à détecter la dysfonction endothéliale.

Nous avons développé une technique de mesure des variations de flot artériel au niveau des membres supérieurs, basée sur la spectroscopie proche infrarouge (NIRS). Cette approche permettrait d'étudier le niveau d'atteinte vasculaire et probablement de quantifier le degré de dysfonction endothéliale périphérique lors d'une hyperémie réactive.

L'expérience a été exécutée sur deux cohortes de 13 et de 15 patients et a été comparée à la pléthysmographie par jauge de contrainte (SGP) qui est considérée comme une méthode de référence.

Par la suite, nous avons caractérisé la réponse endothéliale par modélisation de la courbe hyperémique du flot artériel. Des études préliminaires avaient démontré que la réponse hyperémique adoptait majoritairement une forme bi-modale. Nous avons tenté de séparer les composantes endothéliales-dépendantes et endothéliales-indépendantes de l'hyperémie. La quantification des deux composantes de la réaction hyperémique permet de calculer un indice de la 'santé' du système endothélial local. Cet indice est nommé le *ηfactor*.

Les résultats montrent une forte corrélation des mesures de flots entre la technique développée et la méthode de référence ($r=0.91$). Nous avons conclu que NIRS est une approche précise pour la mesure non-invasive du flot artériel. Nous avons obtenu une bonne répétabilité (ICC = 0.9313) pour le *ηfactor* indiquant sa robustesse. Cependant des études supplémentaires sont nécessaires pour valider la valeur de diagnostic du facteur défini.

Mots clés: hyperémie réactive, réponse myogénique, oxyde nitrique, athérosclérose, spectroscopie proche infrarouge

Acknowledgments

I would like to express my deepest appreciation to my supervisor, Dr. François Harel, who enabled me the chance to pursue an M.Sc. degree at Montreal University in Canada with financial support. To me, it was a dream come true. I deeply acknowledge his knowledge and review of my data and I am fully aware of his support. I can never thank him enough.

I would like to thank my colleague, Quam Ngo, for his contribution to this project as well as his willingness and friendship. I thank Vincent Finnerty for giving me critical and thoughtful comments and the time that he committed for correction of this thesis report.

I would also like to thank Thanh-Thuy Vo Thang who was concerned about me all the time and provided encouragement and friendship. My colleagues from the Montreal Heart Institute including Maryse Bolduc, Sébastien Authier, Sophie Marcil and Matthieu Pelletier-Galarneau helped me in my research work. I want to thank them for all their help.

Finally, I am grateful of my parents and my dearest friend, Soroush, for their support, love and encouragement.

Table of contents

Abstract.....	i
Résumé.....	ii
Acknowledgments.....	iii
Table of contents.....	iv
List of figures.....	vi
List of tables.....	vii
List of abbreviations.....	viii
Chapter 1: Introduction.....	1
Chapter 2: Literature review.....	3
2.1 Blood vessel wall.....	3
2.1.1 Endothelium (<i>intima</i>).....	4
2.1.2 Smooth muscle cells (<i>media</i>).....	9
2.1.3 Nerve endings (<i>adventitia</i>).....	10
2.1.4 Vascular tone regulation stimuli.....	10
2.1.5 Atherosclerosis and endothelial dysfunction.....	15
2.2 Quantification of endothelial function and blood flow measurement.....	16
2.2.1 Non-invasive developed methods.....	17
Chapter 3: Methodologies.....	27
3.1 Instrumentation.....	27
3.1.1 Oxygenation monitor (NIRO-200).....	28
3.1.2 Strain gauge plethysmograph.....	31
3.1.3 Electrocardiograph (AccuSync).....	32
3.1.4 Analog to digital converter (ADC) and RS232.....	32
3.2 Protocol design.....	32
3.3 Experiments setup.....	33
3.4 Blood flow measurement.....	36
3.5 Experiment1.....	37
3.5.1 Subjects.....	37
3.5.2 Protocol.....	38
3.5.3 Setup.....	38
3.5.4 Statistical analysis.....	38
3.6 Experiment2.....	38
3.6.1 Subjects.....	42
3.6.2 Protocol.....	42
3.6.3 Setup.....	43
3.6.4 Data analysis.....	43
3.6.5 Statistical analysis.....	44
Chapter 4: Results.....	45
4.1 NIRS method vs. gold standard (SGP).....	45
4.2 η factor and repeatability.....	48
Chapter 5: Discussion.....	51
5.1 Oxygenation monitor NIRO-200.....	51
5.2 Forearm blood flow.....	51

5.3 Other studies	53
5.4 η factor and its clinical utility	54
5.5 NIRS technique advantages and limitations	56
Chapter 6: Conclusion.....	58
Bibliography:	59

List of figures

Figure 2-1: Blood vessel wall components: intima, media and adventitia.	4
Figure 2-2: Vascular remodeling agents: signals, sensors and mediators [2].....	5
Figure 2-3: The pathway of endothelial derived relaxing factor release [12-14]	7
Figure 2-4: Blood flow during reactive hyperemia, following an ischemic condition.....	14
Figure 2-5: Stages of endothelial dysfunction in atherosclerosis.	16
Figure 2-6: Strain gauge plethysmography.	18
Figure 2-7: Molar absorption coefficients of oxy- and deoxy-hemoglobin in near-infrared region	19
Figure 2-8: Light pathlength in a non scattering (a) and a scattering (b) medium.	21
Figure 2-9: Forearm near infrared spectroscopy.....	22
Figure 2-10: The instrument design of a modular NIRS system by Warier et al.	23
Figure 3-1: Schematic of two measurement modality systems.	27
Figure 3-2: Niro-200 emission and two-segment detection probe.....	30
Figure 3-3: Study protocol timeline.....	33
Figure 3-4: Cuffs position on patient arms during the experiment.	34
Figure 3-5: NIRS probe and strain gauge position.	35
Figure 3-6: Acquisition interface.	36
Figure 3-7: Linear regression application for calculation of arterial inflow with NIRS.	37
Figure 3-8: Blood flow variation during RH measured by NIRSP.....	39
Figure 3-9: Vasoactivation steps during three stages of the experiment.	40
Figure 3-10: Blood flow measurement by NIRSP at three stages of study.	41
Figure 3-11: Gamma variate function fitting on the first and second detected peaks.	44
Figure 4-1: Left forearm blood flow measurements by NIRS and SGP during three stages of experience	45
Figure 4-2: Linear regression between two modalities (SGP and NIRS).....	46
Figure 4-3: Bland-Altman graph of flow measurements with linear regression	47
Figure 4-4: Blood flow measurements during RH by SGP and NIRS.	47
Figure 4-5: Comparison of flow measurements at baseline and post-RH period using paired student's test.....	48
Figure 4-6: One-way ANOVA test showed that there is no significant difference among three repeated groups of measurements	49
Figure 4-7: Linear regression between repeated measurements at t=0 and t=24h.....	49
Figure 4-8: Linear regression between repeated measurements at t=24h and t=27h.....	50
Figure 4-9: No significant difference was shown among the means t_{peak}	50
Figure 5-1: Blood volume variations during venous occlusions by SGP and NIRSP.....	52

Figures 2-1, 2-2, 2-3, 2-5, 2-6, 2-9, 3-1 and 3-9 were produced using *Servier Medical Art*.

List of tables

Table 2-1: Responses of endothelium to mechanical forces including shear stress and stretch..... 8
Table 2-2: Endothelial responses to relatively high and low hemodynamic shear stress 12
Table 3-1: Patient population characteristics for experiment1 38
Table 3-2: Patient population characteristics for experiment2. 42

List of abbreviations

AA	Arachidonic Acid
ACh	Acetylcholine
ADC	Analog-to-digital converter
ATP	Adenosine triphosphate
CAD	Coronary artery disease
cGMP	Cyclic guanosine monophosphate
CNS	Central nervous system
COX	Cyclo oxygenase
DPF	Differential pathlength factor
ECG	Electrocardiogram
EDHF	Endothelial derived hyperpolarizing factors
EDRF	Endothelial derived relaxing factors
FMD	Flow mediated dilatation
Hb	Hemoglobin
ICC	Intraclass correlation coefficient
LBNP	Lower body negative pressure
LDL	Low density lipid
L-NMMA	L-NG-monomethyl arginine
NIR	Near infrared
NIRS	Near infrared spectroscopy
NIRSP	Near infrared spectroscopy plethysmography
NO	Nitric oxide
NOS	Nitric oxide synthase
PGI ₂	prostaglandin I ₂
PLA ₂	Phospholipase A ₂
RH	Reactive hyperemia
sGC	Soluble guanylyl cyclase
SGP	Strain gauge plethysmography
SNS	Sympathetic nervous system

Chapter 1: Introduction

Atherosclerotic diseases are one of the major causes of death and morbidity. Common conditions such as hypercholesterolemia, hypertension, diabetes, and smoking are associated with endothelial dysfunction. These conditions prompt atherosclerosis, indicating the fact that endothelial dysfunction is a premature stage in atherosclerotic diseases, where patients are generally asymptomatic [1].

Endothelium plays a critical role in modulation of the tone of the underlying vascular smooth muscle cells through release of a variety of autocrine and paracrine substances [2]. Importantly, a healthy endothelium inhibits platelet and leukocyte adhesion to the vascular surface, thereby limiting thrombosis.

Nitric oxide (NO) appears to be a particularly important relaxing factor produced by endothelial cells. NO inhibits adhesion and aggregation, maintaining the balance of prothrombotic activity [3, 4]. In patients with coronary diseases, platelet derived NO production is remarkably reduced. This condition is considered as an independent predictor of acute coronary events [5].

Endothelial function has been assessed largely in terms of endothelial dependent vasodilatation, based on the results showing that this response is impaired in patients with atherosclerosis risk factors. This condition can be assessed in catheterization laboratory by coronary intra-arterial infusion of NO agonists, such as acetylcholine (ACh) [6]. Particularly, stimuli that increase production of endothelium-derived NO are used in evaluation of endothelial dependent vasodilatation in humans. Such stimuli include increased shear stress from increased blood flow and infusion of NO agonists such as acetylcholine, bradykinin, or a neuropeptide known as substance P. Several studies have been developed to assess endothelial function non-invasively in peripheral arteries. It has been established that endothelial function in coronary artery is strongly related to that in a peripheral conduit vessel [7].

Strain gauge plethysmography (SGP) is the gold standard method for non-invasive assessment of endothelial function by intra-arterial infusion of ACh [8]. However arterial catheterization for ACh injection is needed in this method. Reactive hyperemia (RH) is a less invasive method to stimulate endothelial cells activation. The technique is based on creation of an acute increase in the limb blood flow through a temporary ischemic condition. The transition state at the release of ischemia induces remarkable amount of shear stress on vascular endothelium that stimulates

release of NO from endothelial cells [9-11]. We used a near infrared spectroscopy (NIRS) device to monitor tissue oxygenation state during reactive hyperemia. The device provides different parameters such as total hemoglobin variations at relatively high sampling rate (6 Hz). We were interested in the relation between oxygenation state and arterial inflow. We assumed that variations in total hemoglobin in terms of time correlate with total blood volume changes.

It was to our interest to evaluate the endothelial function and particularly the NO dependent vasodilatation by monitoring the peripheral arterial flow variations during the reactive hyperemia. Endothelial function assessment results in identification of a group of patients who are relatively at higher risks for cardiovascular events but yet not qualified for medical therapy according to current medical guidelines. This group of patients would benefit from a more aggressive medical or lifestyle treatment.

The purpose of this study is:

- 1) Evaluate the ability of the NIRS device to measure forearm blood flow during reactive hyperemia by comparing to SGP;
- 2) Characterize the function of blood flow variations measured by NIRS plethysmography (NIRSP), during reactive hyperemia.

Chapter 2: Literature review

Heart and blood vessels form the cardiovascular system. Blood vessels play an important role in initialization and development of atherosclerotic vascular diseases. They consist of three different layers through which vascular tone is controlled. Each layer contributes to vascular tone through different mechanisms. Endothelium, which is the inner most layer of blood vessels, has a significant contribution to this regulation.

This chapter presents a brief introduction on different mechanisms of vascular tone regulation along with their effect on blood flow variation. Afterwards, non-invasive methods of blood flow measurement are presented.

2.1 Blood vessel wall

Blood vessels transport blood throughout the whole body. There are three general types of blood vessels: arteries, veins and capillaries. Arteries carry blood away from the heart while the veins carry it back to the heart. Arteries and veins are connected by capillaries, where the exchange of nutrients and chemical wastes is carried out.

Except for capillaries, the two other types of blood vessels consist of three layers: intima, media and adventitia (Figure 2-1).

The intima is a fine layer of endothelial cells in direct contact with circulating blood. Endothelial cells are oriented along the axis of the blood vessels and blood flow. This specific orientation streamlines the endothelial cells to decrease the resistance of the vessels to blood flow.

The media includes smooth muscle cells and is composed of collagen and elastin. It contains terminal nerve endings in some parts, particularly in veins.

The adventitia which is the outermost layer of blood vessels is a fiber elastic layer and it contains terminal nerve endings as well.

Capillaries consist of a layer of endothelial cells surrounded by pericytes that control the vessel diameter.

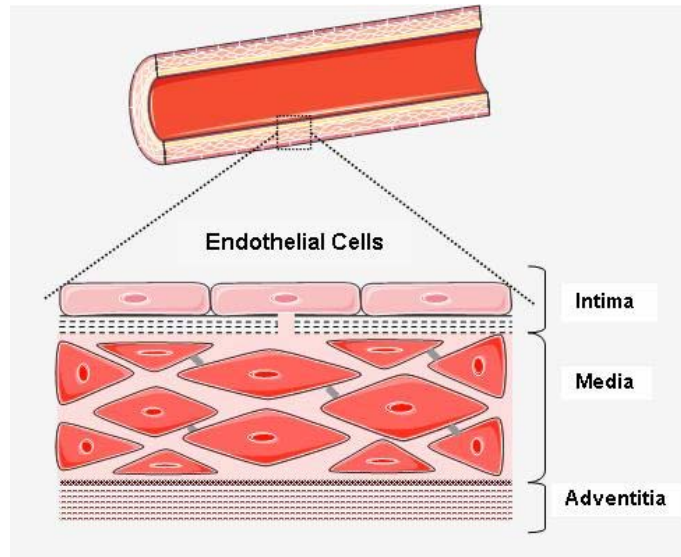


Figure 2-1: Blood vessel wall components: intima, media and adventitia.

2.1.1 Endothelium (intima)

Endothelium is a fine layer of cells in direct contact with circulating blood. It has functional characteristics of an organ as it controls different functions:

- 1) Blood pressure control (through vasoconstriction and vasodilatation),
- 2) Blood fluidity,
- 3) Angiogenesis,
- 4) Synthesis and degradation of extra cellular matrix,
- 5) Inflammation.

The healthy endothelium mediates endothelial dependent vasodilatation along with suppression of thrombosis and vascular inflammation. Therefore, the healthy layer of endothelium is crucial for normal operation of vessels. Endothelium is located strategically to serve as a sensory cell. They participate in vascular remodeling and activation of substances in response to different kinds of physical and chemical stimuli. The pathways mediating the response of endothelium to stimuli are complicated and yet to be fully understood.

The endothelial surface is constantly exposed to two categories of stimuli:

- Chemical substances such as neurotransmitters and inflammatory mediators;
- Hemodynamic forces such as shear stress.

There are a variety of receptors on the surface of endothelial cells to detect physical and chemical stimuli (Figure 2-2). The detected signal is then relayed within the cells and to adjacent cells. In response, endothelial cells release activation substances that influence the cell growth and death, vasodilatation, vasoconstriction and extra cellular matrix composition.

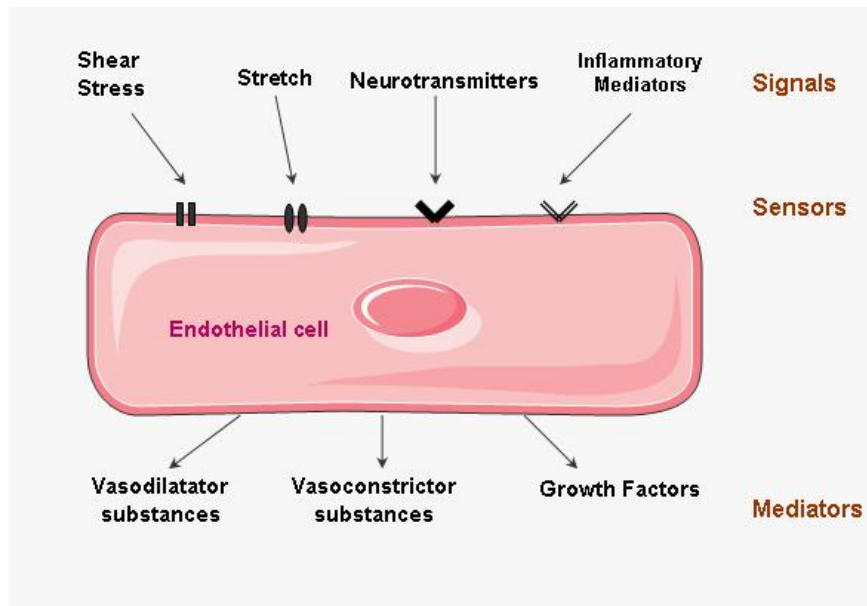


Figure 2-2: Vascular remodeling agents: signals, sensors and mediators [2].

Endothelial cells, as well as smooth muscle cells, are connected via gap junctions.

Endothelial dependent vasodilatation

As vasodilator substances, endothelium releases either relaxing factors, called endothelial dependent relaxing factors (EDRF), or hyperpolarizing factors, called endothelial dependent hyperpolarizing factors (EDHF). Both categories of substances lead to vasodilatation but through different pathways.

Endothelial dependent vasodilatation is triggered by either chemical substances such as acetylcholine, or hemodynamic stimuli such as shear stress. The result is release of EDRF. Nitric oxide (NO) appears to be a particularly important relaxing factor produced by endothelial cells. It is a mediator of endothelium dependent vasodilatation as well as having anti-inflammatory and antithrombotic effect. NO is highly reactive with a half life in the order of a few seconds (2-5 s)

and it diffuses rapidly through cell membranes [3]. Therefore its chemical characteristics make it an excellent agent for short-term and localized responses. NO is synthesized from L-arginine (L-Arg), an amino acid, and oxygen in the presence of enzyme NO synthase (NOS) [4].

Ohno et al. verified the signal transduction pathway of flow induced release of EDRF [12]. Shear stress or the agents with vasoactive properties interact with specific receptors that are located on endothelial cells surface. Consequently, intracellular calcium concentration in endothelial cell increases. Calcium activates NOS, an enzyme that is necessary for NO synthesis. NO reaches other endothelial and smooth muscle cells in the neighborhood. NO in smooth muscle cells stimulates another enzyme sGC (soluble guanylyl cyclase) that synthesizes cyclic guanosine monophosphate (cGMP). Cyclic GMP acts as a second messenger and it activates intracellular protein kinases that mediate smooth muscle cells relaxation and vasodilatation (Figure 2-3). However, the pathway by which protein kinases mediates smooth muscle relaxation remains to be fully understood.

There are other endothelial dependent vasodilator agents other than NO, such as prostacyclin (PGI_2) (Table 2-1).

PGI_2 is another relaxing and anti-thrombosis agent that is released from endothelial cells. Increased calcium activates NOS and phospholipase A_2 (PLA_2) as well. Activated PLA_2 forms prostacyclin metabolism of arachidonic acid (AA) and cyclo oxygenase, (COX)-1.

Mitchell et al. showed that prostacyclin and NO are coreleased from endothelial cells and they act in synergy to inhibit platelet activation and limiting thrombosis [4].

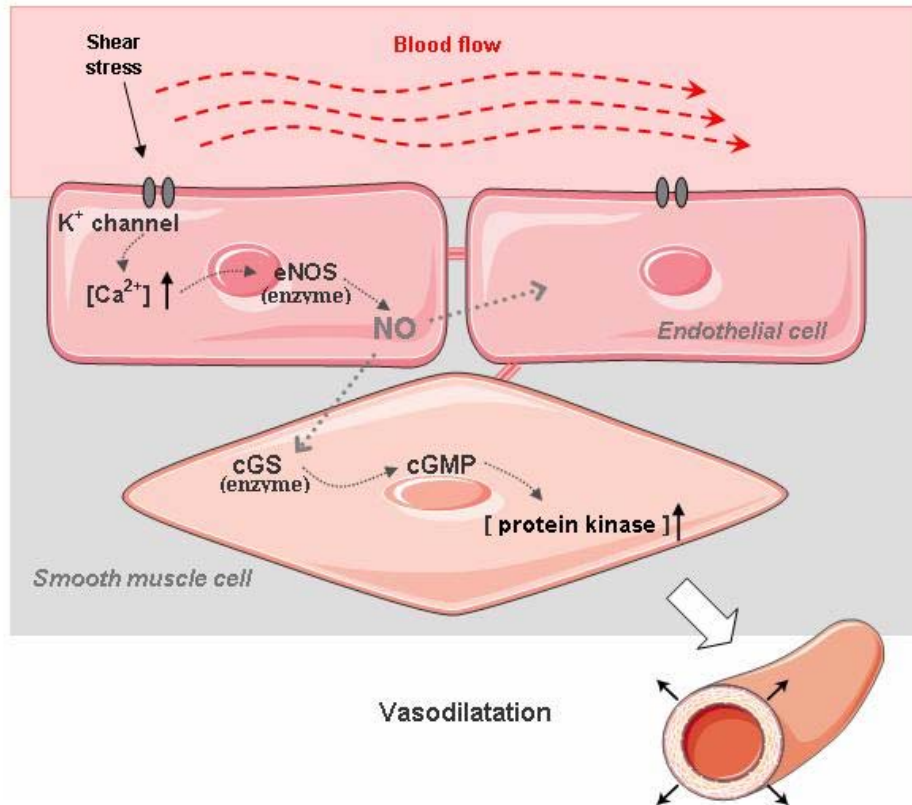


Figure 2-3: The pathway of endothelial derived relaxing factor release [12-14].

There is another relaxant pathway mediated by endothelial cells. EDHF, whose chemical composition is unknown, causes arterial vessels to dilate while NO and prostacyclin productions are inhibited. Potassium channels blocker stops the vasodilatory effect of EDHF, indicating their involvement in the mechanisms of EDHF-mediated vasodilatation. The contribution of EDHF mediated response seems to be greater in smaller vessels [13]. EDHF is known to be released by endothelial cells in response to shear stress but little is known about its mechanism. It seems that the presence of shear stress causes the increase of intracellular calcium concentration in endothelial cells which activates calcium dependent potassium (K_{Ca}) channels. Opening of the endothelial K_{Ca} channels causes potassium ions to be accumulated in the intracellular space between endothelial cells and smooth muscle cells. Increase in myo-endothelial potassium concentration induces hyperpolarization of vascular smooth muscle cells [13]. Table 2-1 summarizes some of the known responses of endothelium to mechanical forces [15].

Mechanical force effects	Significance	Response time
Release of NO	Vasodilatation	secs
Release of acetylcholine and substance P	Neurotransmitter release	secs
Activation of adenylate cyclase	Vasodilatation	mins
Release of prostacyclin (PGI ₂)	Vasodilatation and antithrombotic regulation	< 2 min
Release of EDHF	Vasodilatation	unknown
Release of endothelin	Vasoconstriction	2-4 h
Angiotensin II	Vasoconstriction	unknown
Decrease of intracellular pH	Modulation of ionic balance	> 3 h
Cell alignment in direction of flow	Minimizes drag on endothelial cells	> 6h
LDL metabolism stimulation	Endothelial cholesterol balance	24h
Mechanical stiffness of cell surface	Deformability decrease	24 h

Table 2-1: Responses of endothelium to mechanical forces including shear stress and stretch [15].

Endothelium response to physical and chemical stimuli in subjects with and without atherosclerotic diseases has been studied by many researchers. Anderson et al. compared the endothelial dependent vasodilatation in brachial and coronary arteries in the same patients with various degrees of coronary atherosclerosis [7]. They found that brachial artery is an accessible indicator of endothelium health and the risk of coronary atherosclerosis.

Gokce et al. determined that non-invasive detection of endothelial dysfunction in the brachial artery provides independent prognostic information [16]. They examined flow mediated dilatation (FMD) in patients who were supposed to undergo cardiac surgery up to 1 month before the surgery. They showed that patients with post operative events had significantly lower flow mediated dilatation. They concluded that endothelial dysfunction is an independent predictor of

post operative cardiovascular events and non-invasive assessment of endothelial function in a peripheral artery provides prognostic information.

2.1.2 Smooth muscle cells (media)

The contraction of smooth muscles is mediated through an actin-myosin sliding mechanism that is initiated by calcium binding to myosin. The energy of the process is provided by the hydrolysis of ATP. Vascular smooth muscle contraction and dilatation is responsible for blood volume changes and thus local pressure control. Since arteries carry the blood away from the heart to all the organs, they have more smooth muscle fibers within their walls. Vascular smooth muscle is innervated by the sympathetic nervous system. Three types of receptors (α_1 , α_2 , β_2) are located within vascular smooth muscle cells that cause either vasodilatation or vasoconstriction.

Myogenic response

Vascular smooth muscles are responsible for the establishment of basal vascular tone and autoregulation of blood flow through reaction to chemical and physical stimuli. The myogenic response has been found in all types of vessels. It is most pronounced in arteries but it can be present in venules and veins. It is established that myogenic response is endothelial independent and depends mainly on smooth muscle cells reaction. It has been suggested that pressure-induced changes of vessel wall tension, and not the pressure itself, is the stimulus for myogenic response [14].

Rapid increase in transmural pressure induces an increment in vessel wall tension. Stretch activated cation channels on the surface of smooth muscle cells detect the increase in wall tension and produce membrane depolarization. Depolarization lead to calcium influx and initialization of actin-myosin sliding mechanisms [14, 17].

Calcium influx following an increase in pressure was still present with the removal of the endothelium in a rat experience, indicating the existence of the endothelial independent pathway of vasoconstriction [18]. Pressure step causes the arterioles diameter to decrease and rapidly return to baseline diameter [17, 18].

Another pathway, other than physical stimulus, for vascular smooth muscle cells stimulation are exogenous donors of NO such as sodium nitroprusside and nitroglycerine [7, 16, 19, 20]. Sublingual application of nitroglycerine is widely used in myogenic response studies as an exogenous donor of NO that causes vasodilatation and acts directly on smooth muscle cells.

Anderson et al. demonstrated that coronary response to nitroglycerin was not significantly different between the group of patients with various degrees of coronary atherosclerosis and the control group [7]. Gokce et al. also observed no relationship between nitroglycerine dependent vasodilatation and cardiovascular events [16].

2.1.3 Nerve endings (adventitia)

Adventitia is the outermost layer of blood vessels, innervated by the central nervous system (CNS) that is responsible for several homeostatic mechanism regulations in the human body. The smooth muscles cells activity is controlled via vasomotor neurofibers of the sympathetic nervous system (SNS). The SNS is always active at a basal tone and causes vasodilatation or vasoconstriction according to the organ needs. The transmitters released from nerve endings, such as noradrenalin and adrenaline, bind to adrenergic receptors and alter vascular basal contraction level. The adrenergic receptors of type α_1 and α_2 cause the smooth muscle cells to contract while the receptors of type β_2 cause the muscle cells to dilate. González et al. verified the effect of adventitia removal on vascular function modulation. They demonstrated that contraction capacity of endothelium was reduced by adventitia removal [21]. Hijmering et al. studied the interaction between endothelium dependent vasodilatation and the sympathetic system using lower body negative pressure (LBNP) technique. They found the sympathetic stimulation could impair flow-mediated endothelial-dependent dilatation through a mechanisms caused by adrenergic receptors of type α [19]. They concluded that released transmitters from nerve endings are important modulators of endothelial function and myogenic response.

2.1.4 Vascular tone regulation stimuli

Vascular endothelial cells create an interface between circulating blood and vessel wall. They are exposed continuously to a variety of hemodynamic factors and chemical mediators. The structure and function of blood vessels are influenced by long term exposure to these factors.

1- Shear stress

Shear stress arises from the pulsatility of blood pressure that creates a radial velocity gradient of blood flow through a blood vessel. The velocity of blood particles is at its minimum at the wall of the blood vessels. The shear stress exerted on the vessels walls is function of the velocity profile slope at the wall.

$$\tau_{wall} = \eta \cdot \frac{dV(y)}{dy} \quad (2.1)$$

where τ is the shear stress, η is the blood viscosity, $V(y)$ is the velocity profile along the radial axis y and $dV(y)/dy$ represent the wall shear rate (sec^{-1}). The blood is considered a Newtonian fluid with constant viscosity. In microvessels, where flow rates are relatively steady, shear stress could be expressed as [11, 22]:

$$\tau_{wall} = 8 \times \eta \times \frac{V}{D} \quad (2.2)$$

$$Flow = V \times \pi r^2 \quad (2.3)$$

where V is the blood velocity and r and D are the blood vessel radius and diameter respectively. Shear stress is expressed in dyne/cm^2 . The level of wall shear stress varies in different parts of blood circulation. It varies from 1 to 6 dyne/cm^2 in the venous system and from 10 to 70 dyne/cm^2 in the arterial system.

The nature of shear stress exerted on endothelial cells is a function of blood flow pattern that is itself influenced by cardiac cycles. Therefore, endothelial cells experience a pulsatile shear stress with fluctuation in magnitude. Greater positive shear stress is exerted on endothelial cells surface while the magnitude of fluctuations increase.

The endothelial cells, exposed to positive shear stress, reorient along the longitudinal axis of the vessel wall. This reorientation acts as a negative feedback helping to decrease the vessel resistance and the shear stress [10]. In contrast, in the areas with low mean shear stress, endothelial cells fail to maintain contact with each other and they would be randomly oriented. Malek et al. studied the effect of fluid shear stress on transformation of endothelial cells [23]. They showed that bovine aortic endothelial cells exposed to shear stress of approximately 15 dyne/cm^2 align in the direction of blood flow while those exposed to lower shear stress (0 – 4 dyne/cm^2) were likely to orient randomly.

Ku et al. have measured blood flow velocity and shear stress at the human carotid bifurcation by laser Doppler and under pulsatile flow condition [24]. The medial wall of carotid bulb experiences a higher shear stress compared to the lateral wall. Their study confirmed that plaques tend to form more in the areas experiencing lower shear stress.

Indeed, at the sites with less shear stress, an increase in leukocytes uptake and adhesion on the endothelial cells surface is observable. Steady laminar shear stress causes the endothelial cells to release antithrombotic and antimigration agents. In contrast, reversal flow and lower shear stress promote the release of prothrombotic and pro-apoptosis. Moreover, it is a weaker inducer of NOS. In this condition the production of NO and prostacyclin decreases while the production of endothelin, which is an effective vasoconstrictor, increases [2, 10].

The shear stress effect is exerted through the activation of NOS enzyme and the production of NO. The mechanism involves potassium channels activation as mechanosensory transducer of the shear stress [2, 12]. Table 2 summarizes endothelial response to hemodynamic shear stress based on the Malek et al. study.

Endothelium response	Shear stress > 15 dyne/cm²	Shear stress ≈ 0-4 dyne/cm²
Vasoconstrictors Endothelin Angiotensin	<i>Low</i>	<i>High</i>
Vasodilators NO Prostacyclin	<i>High</i>	<i>Low</i>
Antioxidant enzymes (COX)-1	<i>High</i>	<i>Low</i>
Inflammatory mediators Monocyte chemotactic peptide	<i>Low</i>	<i>High</i>
Thrombosis	<i>Low</i>	<i>High</i>
Endothelial proliferation and apoptosis	<i>Low</i>	<i>High</i>

Table 2-2: Endothelial responses to relatively high and low hemodynamic shear stress [23].

Reactive hyperemia

The creation of shear stress in accessible human blood vessels is a method for endothelial dysfunction evaluation. Reactive hyperemia is a transient increase in blood flow following a period of ischemia. The transition state at the release of ischemia induces a remarkable amount of shear stress on a blood vessels walls (Figure 2-4). Increases in shear stress trigger rapid activation of NOS. This is a widely used method to evaluate the autoregulation capacity of vessel endothelium to return the increased blood flow to the baseline [7, 9, 16, 25]. It has been established that the nature of shear stress is affected by the duration of ischemia. Leeson et al. verified the relation of endothelial dependent vasodilatation and the duration of ischemia. They induced reactive hyperemia with cuff occlusion of 0.5, 1.5, 2.5, 3.5, 4.5 and 8 min. They found that 4.5 minute of cuff occlusion is required to induce a maximal vessel dilatation that arrives one minute after release of cuff occlusion [26]. Mullen et al. demonstrated that L-N-methyl-Arginine (L-NMMA.), the competitive antagonist of NO synthesis, attenuated FMD after a 5 minute occlusion time while after 15 minutes of occlusion, no effect on FMD was observed [27]. It indicates that 5 minute occlusion time induce an endothelial dependent vasodilatation while increasing the duration of ischemia results in an endothelial independent vasodilatation. Another study by Pyke et al. shows that by increasing the duration of shear stress, the FMD response is no longer NO or PGI₂ dependent [11]. Therefore reactive hyperemia created by appropriate ischemia duration induces NO dependent vasodilatation and seems to be an appropriate physical stimulus to evaluate endothelial function.

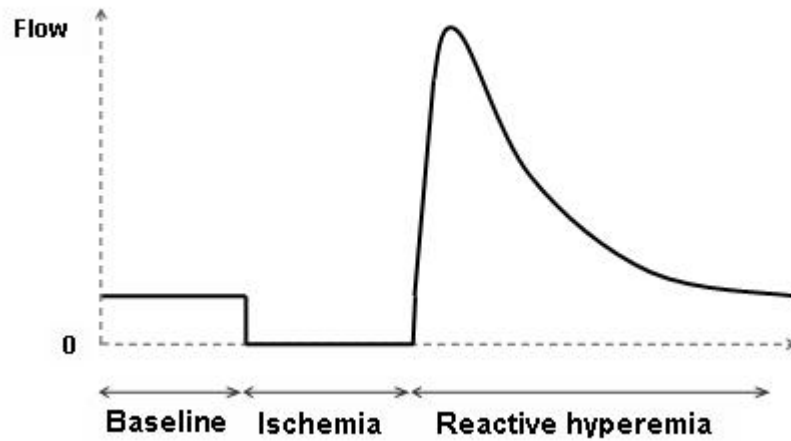


Figure 2-4: Blood flow during reactive hyperemia, following an ischemic condition.

2- Transmural pressure

Transmural pressure is the pressure across the blood vessel walls. In many organs, the blood flow remains at a constant level despite big variations in blood pressure. This vascular autoregulation is mainly due to a pressure induced myogenic response. It is established that in low pressure ranges, 10-40 mmHg, passive distention causes vessel diameters to increase. However, at higher transmural pressures, 60-100 mmHg, active myogenic response results in vessel diameter decrease and vasoconstriction [14]. The sensors that detect the variations of wall tension are stretch activated cation channels. Their activation results in smooth muscle cells membrane depolarization and an increase in calcium influx. Therefore, a steep increase in transmural pressure from 0 to mean arterial pressure, which is the case at the onset of reactive hyperemia, causes an increase in vessel diameter followed by a decrease in diameter due to myogenic response.

3- Agonist agents

There are agonist mediators other than physical stimulus that induce a vasodilatation response. ACh, bradykinin or substance P are endogenous donors of NO that bind to specific receptors on the endothelial cells surface and cause the release of vasodilatory agents such as NO, EDHF and prostacyclin.

Nitroglycerine and sodium nitroprusside are exogenous donor of NO. They convert to NO in the body and they bypass the effect of endothelial cells, thereby inducing direct vasodilatation. Injection of acetylcholine in the arterial vessels and sublingual use of nitroglycerine are widely used methods to evaluate endothelial-dependent and endothelial-independent vasodilatation responses respectively [7]. Eskurza et al. demonstrated that there was a poor correlation between ACh-mediated vasodilatation and shear stress mediated vasodilatation indicating that they provide different information on the endothelial function [28]. It seems that ACh triggers the release of EDHF rather than EDRF (such as NO).

2.1.5 Atherosclerosis and endothelial dysfunction

Atherosclerosis is a chronic inflammatory disease. Atherosclerotic lesions occur principally in elastic and muscular arteries. They develop when low density lipoprotein (LDL) molecules becomes oxidized by oxygen free radicals, which are highly present in arterial blood vessels. The immune system tries to repair the damage created by LDL, by sending leukocytes to the damaged location. However, macrophage blood cells are not able to absorb LDL and they cause extra amount of LDL and leukocyte accumulation within the arterial intima. This process leads to cholesterol plaque creation, remodeling of the artery, decreases of blood flow and shear stress (Figure 2-5).

Accumulation of oxidized LDL in vessel wall results in production of reactive oxygen species. These species are able to rapidly inactivate the production of NO. Most cardiovascular risk factors such as hypercholesterolemia, smoking and hypertension are associated with an increase in oxidative agents, damaging endothelial cells and reduced NO bioactivity [29].

Another important factor in initiation of atherosclerotic lesions is low levels of shear stress at blood vessel wall. The shape and orientation of endothelial cells is influenced by blood flow and shear stress at both intracellular and ultra structural levels. The most important structural manifestation of endothelial cells is their alignment in the blood flow direction. The F-actin filaments are band shaped microfilaments around the periphery of endothelial cells, which are called stress fibers. They are quite important to endothelial cells as they control cells adhesion and shape maintenance. In the region with high levels of shear stress, the stress fibers are aligned with those of neighboring cells. This alignment acts like a single large microfilament extended

on the adjacent endothelial cells able to distribute the shear stress throughout the cells, thereby limiting endothelial cells deformation. These microfilament bundles increase in number when the endothelial cells are exposed to relatively high level of shear stresses. However, in the sites with lower levels of shear stress due to decreased blood flow, endothelial cells adopt a relatively random shape and orientation and show an increase uptake of lipoproteins and leukocytes adhesions on the surface [10, 30].

Uematsu et al. demonstrated a positive correlation between wall shear stress and the extent of microfilament bundle distributions [31]. Their study suggests that low levels of shear stress decrease the formation of microfilament bundles leading to initiation of atherosclerosis.

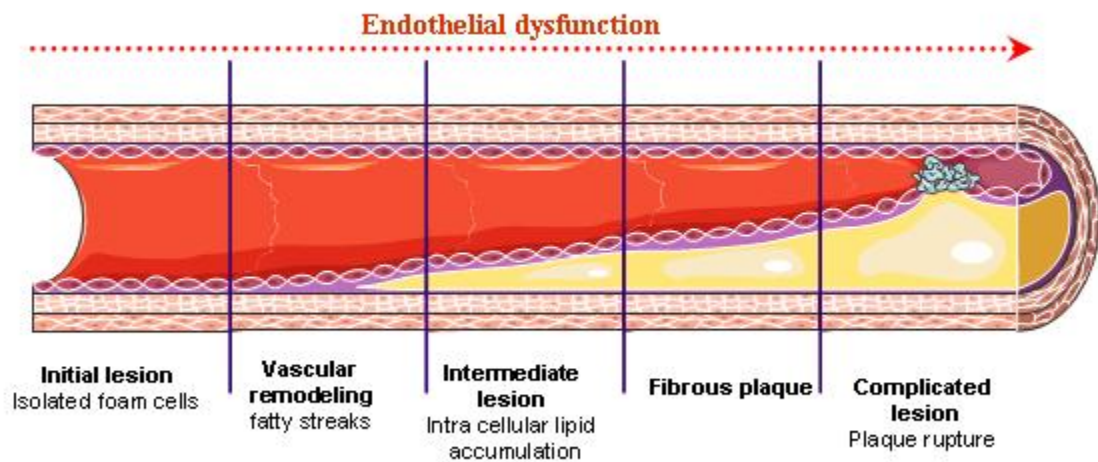


Figure 2-5: Stages of endothelial dysfunction in atherosclerosis.

It is established that endothelial dysfunction is present at very early stages of atherosclerosis and before the disease becomes symptomatic.

2.2 Quantification of endothelial function and blood flow measurement

Reduced bioactivity of NO and enhanced activity of vasoconstrictor agents, in presence of atherosclerotic risk factor, are the main reasons for impaired vasodilator capacity of blood vessels. Vasodilator capacity of endothelial cells could be assessed by measurement of cells response to physical or chemical stimulation that trigger endothelium activation. Endothelium

activation in a healthy vascular system ends up with release of vasodilator agents such as NO and prostacyclin. However, in the presence of atherosclerosis risk factors or an established coronary heart disease, endothelial cells fail to normally respond to an increase in shear stress or endothelial receptors stimulation through releasing relaxing factors.

Several studies have been developed to evaluate endothelial function in patients at high risk for atherosclerosis as well as in patients with already established atherosclerotic disease. A number of invasive and non-invasive methods have been developed. The stimulation of endothelial cells is performed through:

- Agonist receptors stimulation by intra arterial infusion of nitric oxide;
- Shear stress elevation on blood vessel wall through creation of reactive hyperemia.

Vasodilator effect of endothelium on blood vessel wall is evaluated through:

- Measurement of blood flow variations;
- Measurement of flow mediated dilatation (FMD);
- Imaging techniques.

2.2.1 Non-invasive developed methods

In actual clinical situations, coronary endothelial function is assessed using coronary angiography by measuring vasomotor responses to an intra arterial infusion of ACh. However, arterial catheterization limits clinical application of this method in patients with low incident of coronary arterial diseases. Therefore applicable non-invasive methods in patients without known coronary artery seem to be essential in clinical situation. A number of non-invasive techniques with comparable results to invasive methods have been developed. In this section, various non-invasive methods of assessing endothelial function with peripheral arterial vasomotor responses are described.

2.2.1.1 Strain gauge plethysmography (SGP)

Plethysmography is a method to measure volume changes within an organ. Strain gauge plethysmography involves measuring blood volume changes of a limb using a strain gauge. This is an extensively used and accepted method to quantify endothelial function non-invasively, through blood flow measurement [8]. A strain gauge is a stretchable silicone tube containing a

liquid metal such as mercury. The principle of blood volume measurement is based on the theory that the electrical resistance of the mercury filled silicone is directly proportional to its length which varies as forearm circumference change as a response to limb blood volume variations.

Venous outflow is periodically halted and restarted through an inflatable cuff positioned on the upper limb. The cuff is inflated to 50 mmHg to prevent venous outflow without affecting arterial inflow. Consequently the limb swells as the arterial inflow accumulates in venous reservoir and results in an increase of limb volume during cuff inflation. Changes in limb volume are detectable via strain gauges that are placed on the limb. The upslope values of limb volume increase during cuff occlusions and are proportional to the arterial inflow (Figure 2-6).

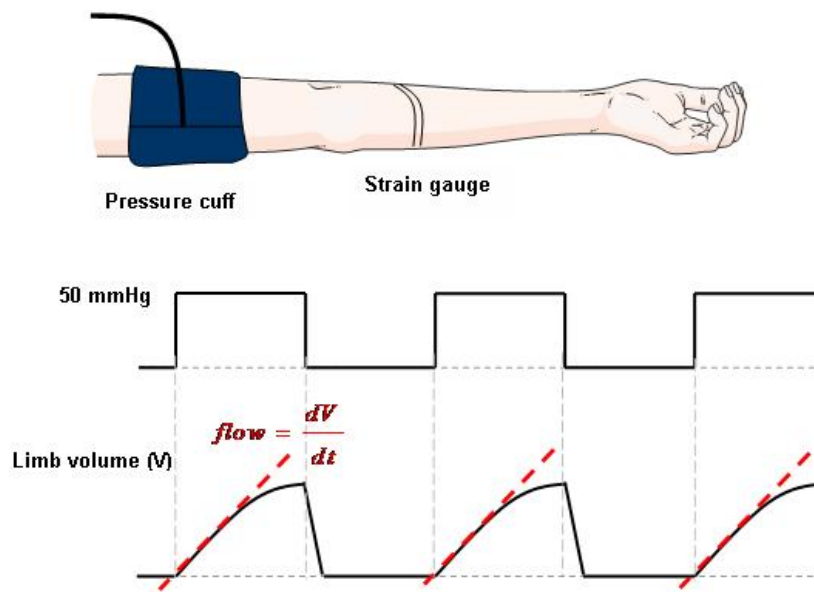


Figure 2-6: Strain gauge plethysmography.

In many reactive hyperemia studies, this technique is used to measure forearm blood flow since it is considered a gold standard method [25]. Measurements are based on the assumption that increment in forearm volume is directly related to limb blood flow. The method is simple and inexpensive which makes its usage feasible for clinical applications. However, it does not provide regional information and should be recorded only in static situation since the technique is very sensitive to any movement of the limb. Therefore, the application of the method in blood flow measurements in dynamic conditions is limited.

2.2.1.2 Near infrared spectroscopy (NIRS)

Near infrared spectroscopy is the measurement of near infrared light (800-2500 nm) intensity and wavelength, absorbed by a sample such as human tissue. NIR light can penetrate relatively far into a sample (up to 6 cm in muscle). Biological tissue is a weak absorber and relatively strong scatterer of NIR light. The absorbed and transmitted light through human tissue contains information about sensitive chromophores (compounds which absorb light in the spectral region of interest) such as hemoglobin and myoglobin molecules, thus permitting the study of physical changes over time.

Each chromophore has its own particular absorption spectrum which describes the level of absorption at each wavelength (Figure 2-7).

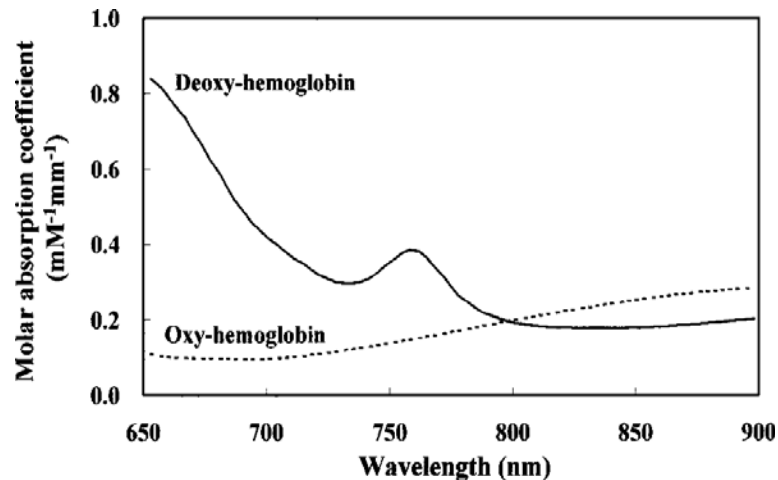


Figure 2-7: Molar absorption coefficients of oxy- and deoxy-hemoglobin in near-infrared region measured by Yamashita et al. [32].

Wavelengths within the near infrared region seem to be suitable for the measurement of hemoglobin due to their relatively deep penetration. The wavelength region of 750 – 850 nm is widely used for non-invasive measurement of oxy and deoxy hemoglobin concentration since the two spectra intersect around a wavelength of 805 nm that provides a measurement independent of the degree of hemoglobin oxygenation allowing total hemoglobin concentration measurement [32]. The variations in the total hemoglobin reflect variations in the blood volume. Therefore, blood flow can be calculated by relative changes of total hemoglobin from the baseline at a given time. NIRS monitors oxygen as a tracer.

The principle of measurement

The relation between light absorption and chromophore concentration in a non scattering medium is described by Beer Lambert law:

$$A = \log \left(\frac{I}{I_0} \right) = d \cdot \alpha \cdot c \quad (2.4)$$

where A is light attenuation, I and I_0 are incident and transmitted light intensities respectively, α is the absorption coefficient, c is the chromophore concentration and d is the distance that light travels through the sample (physical distance between light emitter and detector). However, in a scattering medium such as biological tissue, light do not travel in a direct path and thus light attenuation is a complex function of tissue geometry, absorption and scattering coefficients. Therefore, the modified Beer Lambert law is expressed to take these variables into account:

$$A = \log \left(\frac{I}{I_0} \right) = L \cdot \alpha \cdot c + G \quad (2.5)$$

where L is the actual light pathlength which is not straight due to scattering ($L > d$), G is the light attenuation due to scattering that is an unknown parameter. Because of the later factor (G), the equation can not be solved to yield an absolute concentration of the chromophore. However, if G is considered as a constant parameter in terms of time, it is possible to measure relative variations of the chromophore concentration, oxy and deoxy hemoglobin (Figure 2-8).

$$\Delta A = L \cdot \alpha \cdot \Delta C \quad (2.6)$$

Changes in C can be calculated relative to a starting point considered as zero.

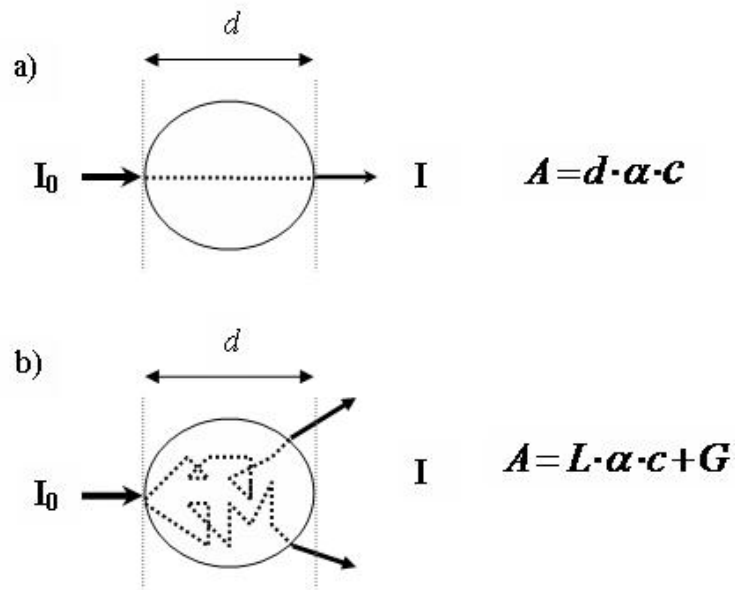


Figure 2-8: Light pathlength in a non scattering (a) and a scattering (b) medium.

The differential pathlength factor (DPF), which indicates light pathlength through tissue is measured by time resolved spectrometry method that is based on the measurement of time of ultrasound pulses flight through a tissue.

$$L = \frac{c \cdot t}{n} \quad (2.7)$$

where c is sound speed and n is refractive index of tissue.

The modified Beer Lambert law is used for the measurement of relative variations in oxy and deoxy hemoglobin. The variations in total hemoglobin concentration correlate with variations in total blood volume, an assumption required for the measurement of blood flow [33].

NIRS probes have a special optical design. The emission probe radiates laser beams in NIR region and the detection probe detects attenuated light that has passed through the tissue of interest. The emission probe is made of fiber optics and the detection probe is a photodiode sensor (light to current converter) which is placed some centimeters apart from the emission probe. The emitted light illuminates the tissue in a ‘banana-shaped’ distribution providing information from relatively deep tissue layers. In human oxygenation measurements, the detection probe is usually placed on the same side and not on the opposite side. In this particular case, it detects a part of the diffused and reflected light (Figure 2-9).

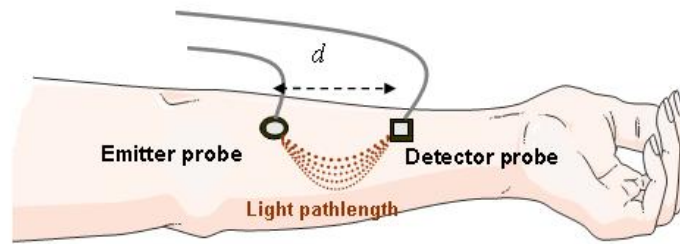


Figure 2-9: Forearm near infrared spectroscopy.

The distance between emitter and detector is a compromise between received light intensity and deeper light traveling. In fact when the emitter-detector separation increases, the detected light intensity decreases while it carries more information from deeper layers of tissue. Therefore, specific emitter-detector separation provides information from specific layer of the tissue of interest. This separation is usually chosen to be between 2 and 3 cm [34, 35].

Yu et al. studied the dynamics of muscle blood flow during reactive hyperemia using NIRS [36]. They tried different source-detector separation configurations. They found that increase in source-detector separation causes an increase in blood flow and blood oxygen saturation overshoots following cuff occlusion while oxygen saturation undershoot during ischemia decreased.

Wariar et al. constructed a modular NIRS system for clinical measurement of impaired skeletal muscle [37]. Their system design leads to an understanding of the basis of an NIRS system. Elements of their systems are showed as a block diagram in Figure 2-10.

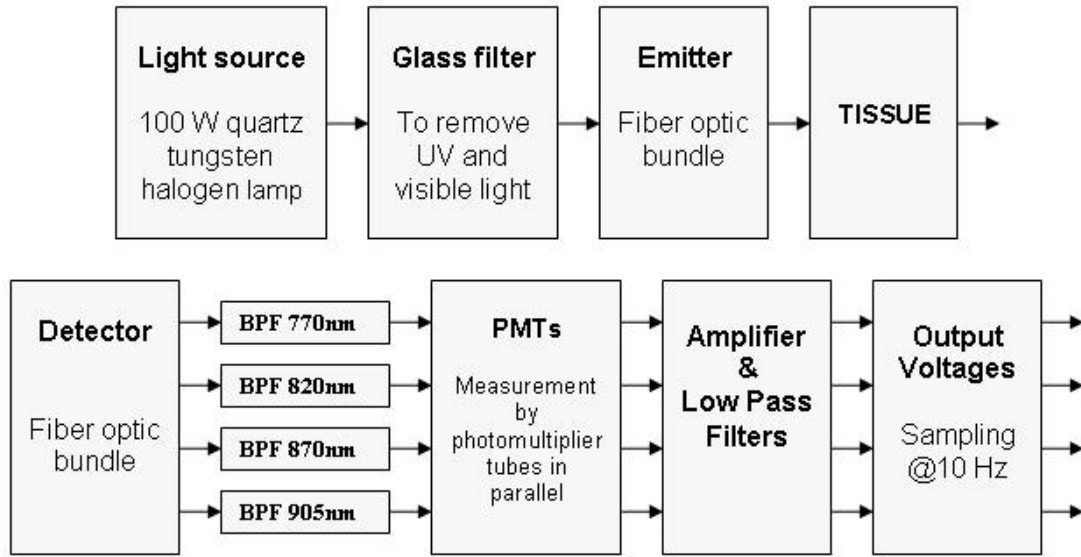


Figure 2-10: The instrument design of a modular NIRS system by Wariar et al. BPF represents band-pass filter [37].

They calculated variations in optical absorption at each wavelength from the logarithm of the measured output voltages ratio:

$$\Delta A(t) = -\Delta \log(V_o - V_{dark}) = -\log \frac{V_o(t) - V_{dark}}{V_b - V_{dark}} \quad (2.8)$$

where V_{dark} is voltage output without any illumination source and V_b is voltage of forearm at rest before any occlusion or activity. Changes in absorption are then converted to changes in concentration of oxy- and deoxy- hemoglobin.

$$\Delta A_\lambda = \sum \alpha_\lambda \cdot \Delta C \cdot d \quad (2.9)$$

2.2.1.3 Other methods

Pulsed Doppler Ultrasound

This echography approach provides both blood vessel image and the velocity of the blood in the artery. Volume blood flow can be measured in deep abdominal vessels using this technique [38, 39]. The technique is based on the Doppler effect which corresponds to an alteration in sound

wave frequency resulting from the motion of red blood cells. The velocity of red blood cells is given by:

$$V = \frac{\Delta f_{\max} \cdot c}{2 \times f \cdot \cos \theta} \quad (2.10)$$

where f is the transmitted frequency, c is the sound speed and θ is the angle between the sound beam and the blood flow direction. The volume flow rate is calculated by:

$$Flow = V \cdot A \quad (2.11)$$

where V is the mean velocity and A is the cross-sectional area of the blood vessel determined from the ultrasonic image of the blood vessel. The penetration depth of ultrasound waves is a function of incident wave frequency. For example, 8 MHz probe provides penetration depth of 4 cm for ultrasound wave. Therefore, superficial structures are imaged at a higher frequency (8-18 MHz) while deeper structures are imaged at a lower frequency (1-7 MHz).

Shear stress and flow mediated dilatation (FMD) that describes the vasodilatory response of a vessel to blood flow elevations are measured using the ultrasound image of the vessel as following:

$$FMD(\%) = \frac{D_{DF} - D_{BL}}{D_{BL}} \quad (2.12)$$

$$SS = 8 \times \mu \times \frac{V}{D_{BL}} \quad (2.13)$$

where D_{BL} and D_{DF} represent brachial artery diameters at baseline and post-deflation phases respectively, SS represents shear stress, V is blood flow velocity and μ is blood viscosity. The technique provides flow changes measurement in deeper tissue layers. However, it is not sensitive to blood flow in small vessels such as capillaries and arterioles and it does not provide continuous measurement.

Laser Doppler

This is a non-invasive technique for measurement of red blood cells perfusion in tissue [40]. A percentage of light beam incident in tissue is scattered by moving red blood cells that results in a frequency shift of the light. The light which is backscattered by red blood cells, as well as by static tissue, is detected by a photodetector. The emitted and returned light are then compared to

extract the Doppler shift caused by moving red blood cells. The Doppler shift is proportional to the flux of red blood cells.

The technique provides a continuous recording at the region of interest. However, it is only able to measure flow changes at the surface level since the penetration depth of the laser beam is no greater than 500 μm [41].

Magnetic resonance imaging (MRI)

MRI is an extremely versatile technique that provides anatomical and functional information on a body region of interest. The technique has wide applications in quantitative assessment of blood flow and blood oxygenation [42, 43]. Oxygenated and deoxygenated hemoglobin are diamagnetic (negative magnetic susceptibility) and paramagnetic (positive magnetic susceptibility) respectively. Increase in blood flow is accompanied with an oxy-hemoglobin concentration increase and a deoxy-hemoglobin concentration decrease. Therefore, the magnetic susceptibility decreases resulting in MRI signal intensity enhance.

The technique provides high temporal and spatial resolution images. However, the large size and high cost of MRI systems restrict their clinical applicability in reactive hyperemia studies.

Positron emission tomography (PET)

PET is a nuclear medicine imaging technique which provides a map of metabolic process in the body that allows the study of biochemical changes in terms of time. The technique is used for assessment of blood flow in peripheral vascular disease. After intravenous bolus injection of ^{15}O -water (H_2^{15}O) radioactive molecules, a dynamic PET scan is acquired. Time-activity curves in blood and tissue reflect different regional blood flow [44]. Compared to MRI, the technique provides poor spatial and temporal resolution while it is also costly.

Radionuclide plethysmography

Radionuclide plethysmography is a recently developed and validated method by Harel et al. in the nuclear department of Montreal Heart Institute [45, 46]. Radionuclide plethysmography uses gamma detector probes to detect radioactivity variation during repeated venous occlusions. The method uses technetium-99m ($^{99\text{m}}\text{Tc}$) labeled autologous red blood cells as radioactive tracers to measure the radioactivity variations. The $^{99\text{m}}\text{Tc}$ compound with red blood cells can be used to

map circulating blood in an organ such as the forearm. Measurements performed with this method were highly correlated with those performed with SGP. However, intra arterial injection of a radioactive tracer is needed.

Chapter 3: Methodologies

We designed two experiments to test our hypotheses. The first experiment (Experiment1) was designed to test the ability of NIRS to measure blood flow variations in the forearm during reactive hyperemia. The second experiment (Experiment2) was designed to characterize the contribution of endothelium in vascular tone regulation during reactive hyperemia. Instrumentation, protocol designs and setup as well as the method of blood flow calculation that are common to both experiments are described in sections 3.1 to 3.4. Analyses that are specific to each experiment are described in sections 3.5 and 3.6.

3.1 Instrumentation

Figure 3-1 shows the schematic of all instruments including a strain gauge plethysmograph system, an NIRS system, an occlusion system, an electrocardiograph, an A/D converter and a computer.

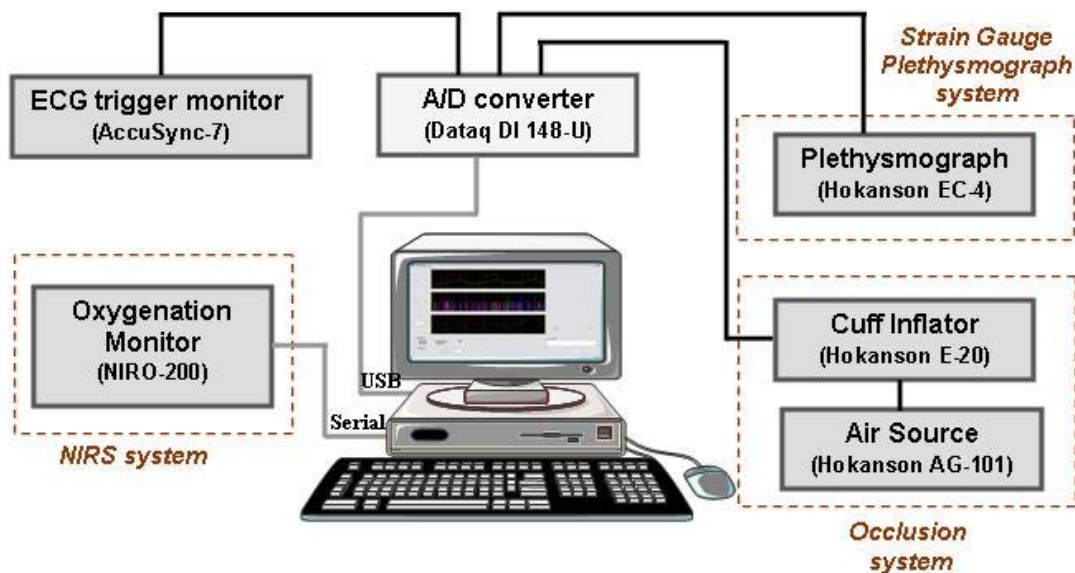


Figure 3-1: Schematic of two measurement modality systems.

3.1.1 Oxygenation monitor (NIRO-200)

The Niro-200 is a tissue oxygenation monitor based on near infrared spectroscopy. It provides continuous, non-invasive and real-time measurement of tissue oxygenation with a sampling rate of 6 Hz. The device is useful in clinical studies such as metabolism and function of brain as well as the study of muscle tissue oxygenation. Niro-200 is a two-channel oxygenation monitor allowing simultaneous measurement at two sites. It provides six parameters:

- Changes of oxygenated hemoglobin (ΔO_2Hb)
- Changes of deoxygenated hemoglobin (ΔHHb)
- Changes of total hemoglobin (ΔcHb)

$$\Delta cHb(t) = \Delta HHb(t) + \Delta O_2Hb(t) \quad (3.1)$$

- Ratio of oxygenated to total hemoglobin in percentage (TOI)

$$TOI(t) = 100 \times \frac{O_2Hb(t)}{cHb(t)} \quad (3.2)$$

- Relative value of total hemoglobin (THI)

$$THI(t) = k \times cHb(t) \quad (3.3)$$

k : a constant that is determined by the light scattering property in the measured tissue

- Normalized THI by the initial value ($nTHI$)

$$nTHI(t) = \frac{THI(t)}{THI(0)} \quad (3.4)$$

The light source is a pulsed laser diode with a pulse duration of approximately 200 ns and a frequency of 2.7 kHz. The detection probe is a photodiode. Optical fiber bundles transfer the light produced by the light source to the emission probe and a multiwired shielded cable carries back the detected light to the device for analysis.

Measurement principle

The modified Beer Lambert law is used for the measurement of ΔO_2Hb , ΔHHb and ΔcHb . The light attenuation variations at three wavelengths (775, 810, 850 nm) are calculated for

measurement of three unknown parameters: ΔO_2Hb , ΔHHb and pathlength (L). In fact the calculation of the three parameters is based on light attenuation in terms of time.

$$\begin{aligned}
 \Delta A(\lambda_1) &= L \times [a(1,1) \times \Delta O_2Hb + a(2,1) \times \Delta HHb] \\
 \Delta A(\lambda_2) &= L \times [a(1,2) \times \Delta O_2Hb + a(2,2) \times \Delta HHb] \\
 \Delta A(\lambda_3) &= L \times [a(1,3) \times \Delta O_2Hb + a(2,3) \times \Delta HHb]
 \end{aligned} \tag{3.5}$$

where $a(i, j)$ represents molar extinction coefficient of HHb and O_2Hb ($i=1, 2$) at wavelengths (λ_1, λ_2 and λ_3). If the pathlength is known in the above equations, ΔO_2Hb and ΔHHb are calculated as absolute concentration changes ($\Delta \mu\text{mol}$). It seems to be established that if physical distance between emitter and detector (d) is more than 3 cm, the pathlength is proportional to the distance by a constant called differential pathlength factor (DPF).

$$L = DPF \times d \tag{3.6}$$

The NIRO-200 operation manual provides typical DPF values for different parts of the body such as the forehead, the forearm and the calf in males and females. Since the value of physical distance (d), between detector and emitter for Niro-200 is 4 cm, it is possible to estimate the pathlength and input it into the device setting function.

$$L(\text{forearm}) = 3.59 \times 4\text{cm} = 14.36\text{cm}$$

TOI and THI are measured using spatially resolved spectroscopy method. In this method, light attenuation is measured along distance ($\partial A / \partial \rho$). The Niro-200 employs a two segment photodiode chip to measure light attenuation along the distance between the two segments (Figure 3-2).

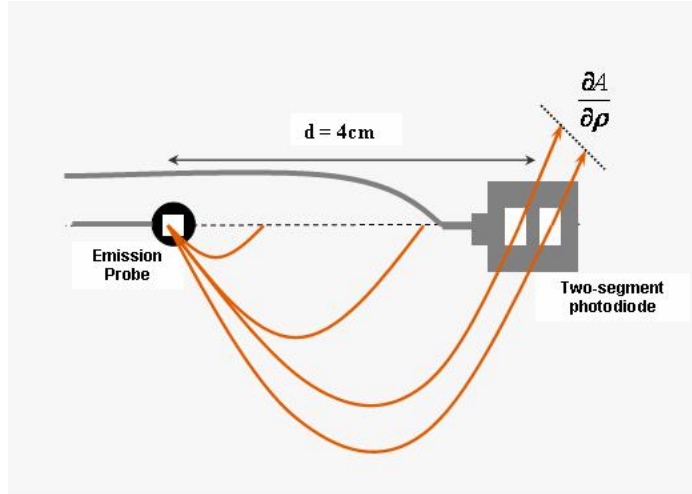


Figure 3-2: Niro-200 emission and two-segment detection probe.

The value of $\frac{\partial A}{\partial \rho}$ is calculated at three wavelengths by an equation derived from the photon diffusion principle.

$$\begin{aligned}
 \frac{\partial A(\lambda_1)}{\partial \rho} &= \sqrt{k \cdot \{a(1,1) \times O_2Hb + a(1,2) \times HHb\}} + \frac{2}{d} \\
 \frac{\partial A(\lambda_2)}{\partial \rho} &= \sqrt{k \cdot \{a(1,2) \times O_2Hb + a(2,2) \times HHb\}} + \frac{2}{d} \\
 \frac{\partial A(\lambda_3)}{\partial \rho} &= \sqrt{k \cdot \{a(1,3) \times O_2Hb + a(3,2) \times HHb\}} + \frac{2}{d}
 \end{aligned} \tag{3.7}$$

where k is the unknown parameter determined by light scattering properties.

Light pathlength

Adequate infrared light penetration into tissue is an important issue. The depth of light penetration depends on optical tissue properties as well as source-detector separation. The muscle layer lies generally under the skin and adipose tissue (upper layer). The thickness of the upper layer is in the order of a few millimeters.

It has been established that signal from short source-detector separation (0.5-1 cm) are derived mainly from upper layers whereas signals detected from detector separated more than 2 cm from the source are mostly due to the muscle layer [36]. However, there is always a contribution from the upper layers to the detected signal. The distance between the Niro-200 emission and

detection probes (4 cm) seems to be sufficient to make the infrared light travels deep enough in the tissue to remove the contamination from the superficial layer.

3.1.2 Strain gauge plethysmograph

A venous occlusion plethysmograph system consists of the following parts:

- Limb strain gauge
- Plethysmograph
- Rapid cuff inflator
- Cuff inflator air source
- Pressure cuffs

In our experiments, strain gauge plethysmography was performed using a dual-channel plethysmograph (Hokanson EC-4, D.E. *Hokanson* Inc). The plethysmograph is able to detect very small changes in limb volume, providing precise monitoring of forearm blood volume variations. On the other hand, its sensitivity makes the signals vulnerable to artifacts. The analog output of the plethysmograph is transferred to a PC via an analog to digital (A/D) converter.

Different forearm gauge sizes from 16 to 32 cm are available to accommodate the patient's forearm size. The gauges are placed on the forearm 5 cm below the elbow. They have double rubber loops, filled with mercury that wrap in parallel around the limb. As the volume of the limb changes, the gauge tube is stretched and the electrical resistance varies proportionally to the volume size. Resistive variations are processed and displayed as waveforms expressed in $\text{mL} \cdot \text{dL}^{-1} \cdot \text{min}^{-1}$

The *Hokanson* E20 rapid cuff inflation system was used to inflate the pressure cuffs, used for venous and arterial occlusions. It can inflate and deflate the vascular cuff in less than 0.3 seconds over a range of 0 to 300 mmHg as well as maintaining the pressure for as long as the protocol requires. The E20 digital readout displays cuff pressures within 1 mmHg over a range of 0 to 300 mmHg. The E20 requires a source of pressurized air provided by the *Hokanson* AG101.

3.1.3 Electrocardiograph (AccuSync)

A 3 lead ECG trigger monitor (AccuSync 7, Medical Research Corporation, Milford) displays the ECG of the patient and automatically detects the R waves. The ECG signal and R triggers are recorded on the computer for further analysis of a patient's cardiac rhythm variation during the experience.

3.1.4 Analog to digital converter (ADC) and RS232

The SGP and ECG signals are transferred to the computer via an A/D device (Dataq, model DI-148U, DATAQ Instruments, Inc., Akron, Ohio) at 250 Hz. The 8 channel ADC power is derived from the PC through the USB interface. The voltage resolution of the converter is ± 19.5 mV (10 bits) with a full scale measurement range of -10 to +10 volts. The maximum sampling frequency of the ADC is 14,400 Hz. In addition, the NIRS signal is transferred to the computer via an RS232 port.

3.2 Protocol design

In both experiments, the protocol included three consecutive stages (Figure 3-3).

- Baseline or pre-ischemic period (3 min),
- Ischemic period (5 min),
- Reactive hyperemia or post-ischemic period (7 min).

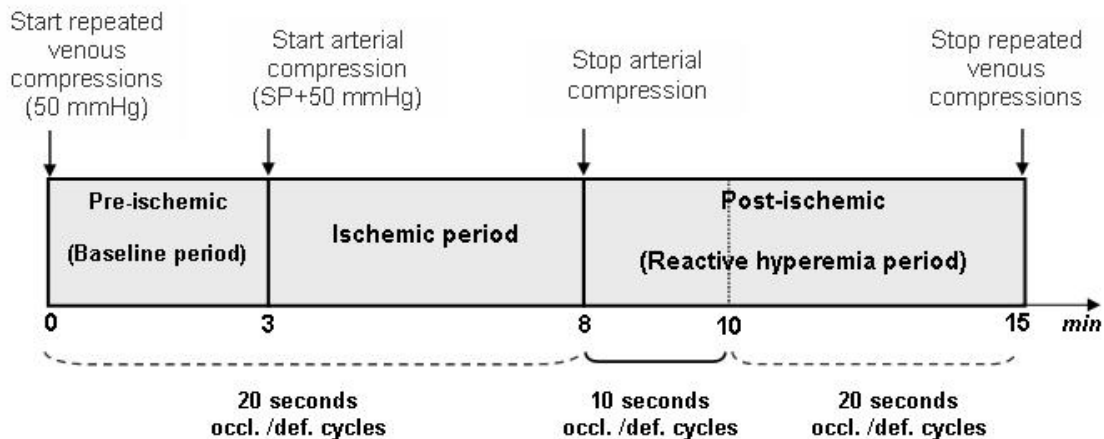


Figure 3-3: Study protocol timeline (*SP* represents systolic pressure).

The blood flow measurements were made by successive cycles of venous occlusion and release during the experiment. At the baseline, flow measurements were performed with 20 seconds occlusion-deflation cycles (10 sec occlusion time followed by a 10 sec deflation time). The pressure was applied through a pressure cuff (venous cuff) connected to the pneumatic cuff inflator. Nine measurements were obtained during 3 minutes of pre-ischemic period.

After this period, a suprasystolic pressure was applied through another cuff (arterial cuff), on the left arm for 5 minutes to halt forearm blood circulation. During the ischemia period, 15 flow measurements were obtained. After 5 minutes of ischemia, arterial cuff was released to evoke hyperemic response on the left forearm. Successive cycles of venous cuff occlusion-deflation were decreased to 10 seconds for the first 2 minutes post-ischemic to obtain a higher temporal resolution. During the post ischemic period, 27 inflation-deflation cycles were performed resulting in 27 flow measurements.

3.3 Experiments setup

The experiment was carried out in a quiet room with a temperature of 24° C. Patients sat in supine position on a recliner chair with arms prone and above heart level in order to facilitate the venous outflow. Venous cuffs were placed around distal parts of left and right upper arms to

perform repetitive venous occlusions. Both cuffs were connected to a pneumatic cuff inflator set to 50 mmHg. This cuff pressure is sufficient to occlude completely the venous outflow without affecting arterial inflow [47].

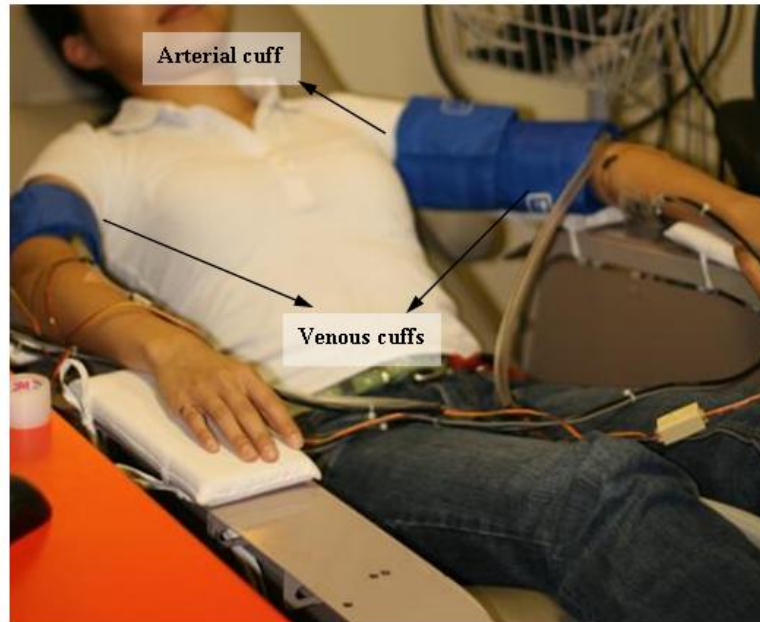


Figure 3-4: Cuffs position on patient arms during the experiment.

The Arterial cuff was placed on the proximal part of the left upper arm (Figure 3-4). The cuff was inflated to a pressure of 50 mmHg above systolic pressure. The duration of arterial occlusion is an important issue for inducing maximum endothelial cells stimulation and as a result, vessel dilatation. It has been shown that maximum arterial response is reached after 4.5 min of occlusion [26]. Occlusion cuff position is also an important determinant of the magnitude of brachial artery flow-mediated dilatation. It seems to be established that upper arm cuff placement yields greater hyperemic response compared to wrist cuff placement [48, 49]. Therefore, upper arm occlusion is more suitable for detection of subtle differences between groups of patients.

Strain gauges were placed around the largest part of the left and right forearms (about 5 cm below the elbow crease) and were connected to the plethysmograph. NIRS sensors were placed on the anterior parts of the left and right forearms adjacent to the strain gauge in a longitudinal

orientation and at approximately the same distance from elbows. They have auto-adhesive surface to hold firmly on the forearm skin and preventing any displacement (Figure 3-5).

The electrocardiogram (ECG) was recorded using 3 leads throughout the experiment to detect any cardiac cycle variations during different phases of the experience.

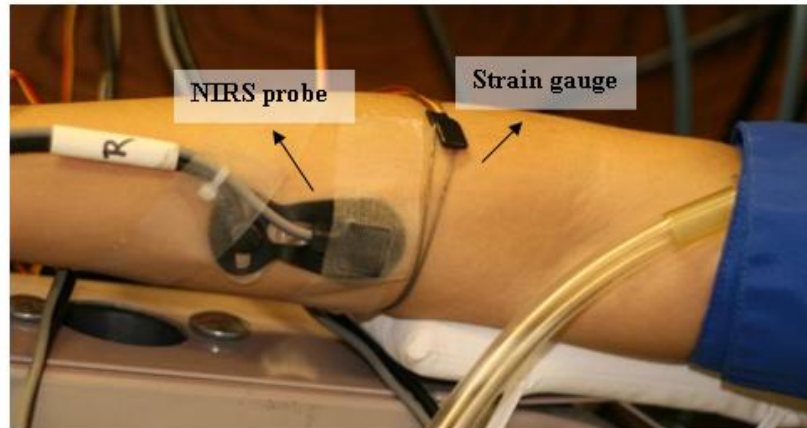


Figure 3-5: NIRS probe and strain gauge positions.

All signals including blood volume variations in mL/100mL/min by SGP, total hemoglobin variations in $\mu\text{mol/L}$ by NIRS and electrocardiograph with time based control codes were recorded on a personal computer by a custom acquisition program designed with the MATLAB[®] programming language (Figure 3-6). For an online signal quality monitoring, the signals were plotted in real time throughout the experiment.

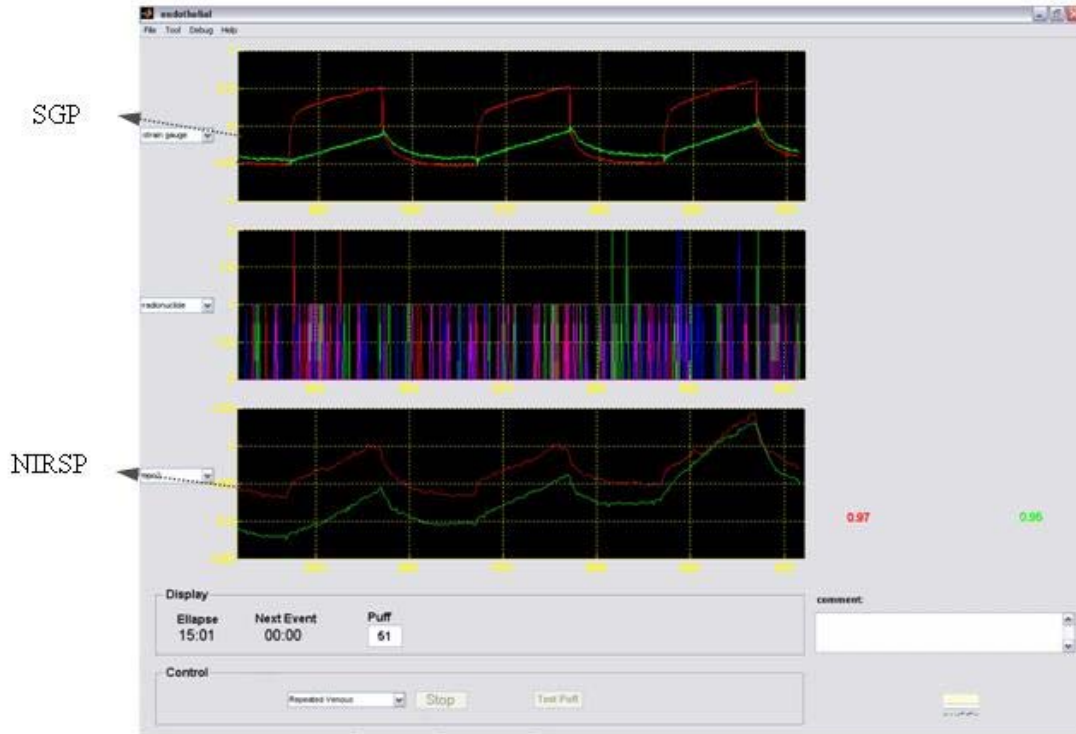


Figure 3-6: Acquisition interface.

3.4 Blood flow measurement

The increase in blood volume generated by the application of repeated venous occlusions, allows the computation of the arterial inflow. It is defined as:

$$flow = \frac{d(Volume)}{dt} \quad (3.8)$$

The arterial inflow was calculated for each venous occlusion by computing the upslope value on the ascending part of blood volume variations. Repetitive venous cuff inflation and deflation caused slight movements of forearms all throughout the experience. These movements affect SGP signal through sharp rises at the onset of cuff inflation (cuff jump). In order to avoid blood flow overestimation, we excluded the first 2 sec of SGP signal from upslope calculation. We applied a linear regression model on the next 3 seconds period of the signal to calculate the rate of blood volume increase at the onset of each venous occlusion (Figure 3-7). Although the NIRSP signal was almost unaffected by the mentioned artifact, we considered the same period of time as SGP for the flow measurement.

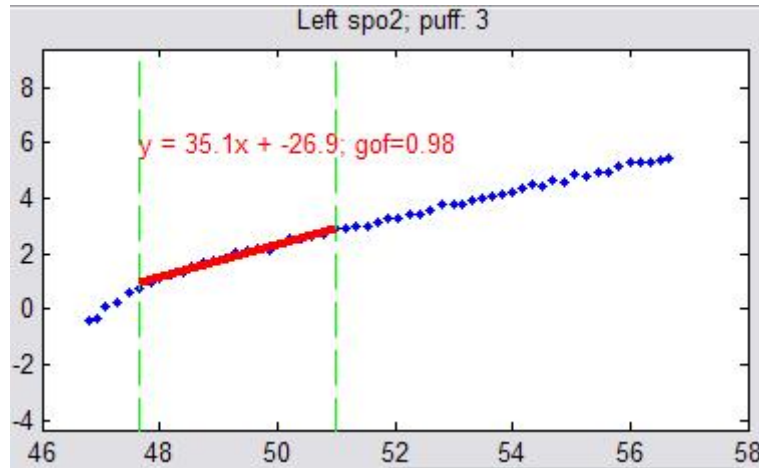


Figure 3-7: Linear regression application for calculation of arterial inflow with NIRS.

The SGP measures blood relative volume variations in limbs (in mL of blood/100mL of tissue). The application of linear regression provides the rate of relative blood volume variations thus the arterial inflow in $\text{mL} \cdot 100\text{mL}^{-1} \cdot \text{min}^{-1}$.

By NIRSP, we are able to indirectly measure arterial inflow. The NIRS device provides total hemoglobin variations in $\mu\text{mol/L}$, which is proportional to blood volume variations. Upslopes were calculated using a linear regression model. Therefore, we obtained arterial inflows in $\mu\text{mol/L}/\text{min}$. In order to provide arterial inflow measurements in the same units as SGP ($\text{mL}/100\text{mL}/\text{min}$), we applied a calibration factor on the flow measures by NIRSP. A linear regression between blood flow measurements during reactive hyperemia, by SGP in $\text{mL}/100\text{mL}/\text{min}$ and NIRS in $\mu\text{mol/L}/\text{min}$ was performed. The Slopes of the regression fit was used as the calibration factor.

3.5 Experiment 1

3.5.1 Subjects

After the protocol approval by the research and ethics committees of the Montreal Heart Institute, 13 healthy volunteers with a low likelihood of coronary artery disease (CAD) were recruited for the experiment (Table 3-1) [50].

<i>Gender</i>	5 men / 8 women	
<i>Age</i>	40 ± 14	
<i>BMI</i>	28.2 ± 3.8 kg/m ²	
<i>Patients condition</i>	Active smoker	<i>n=1</i>
	High blood pressure	<i>n=1</i>

Table 3-1: Patient population characteristics for experiment1.

3.5.2 Protocol

The protocol of the experience was the same as the previous study described in 3.1.

3.5.3 Setup

SGP and NIRSP measurements were performed simultaneously during the experiment and the experiment setup was the same as described in 3.2.

3.5.4 Statistical analysis

Statistical analysis was performed using the SPSS statistical package version 10.0 and GraphPad Prism version 5.01. We evaluated the repeatability of measurements at baseline through intra-class correlation coefficient (ICC) at baseline level for each modality. Nine measurements were made during baseline period. To understand the relation between forearm blood flow measurements during reactive hyperemia, we performed a linear regression. Bland-Altman plot allowed the verification of the agreement between the two methods. We used repeated ANOVA test to verify the existence of a significant difference between the two modalities during reactive hyperemia. Statistical significance was accepted when the two-tailed p value was <0.05.

3.6 Experiment2

We found a good correlation between flow measurements by NIRSP and SGP [51]. Blood flow measurements during reactive hyperemia allowed to isolate the flow mediated dilatation following an acute increase in blood flow. We were interested in studying the integrity of the

endothelium using blood flow variations measured by NIRSP during reactive hyperemia (Figure 3-8).

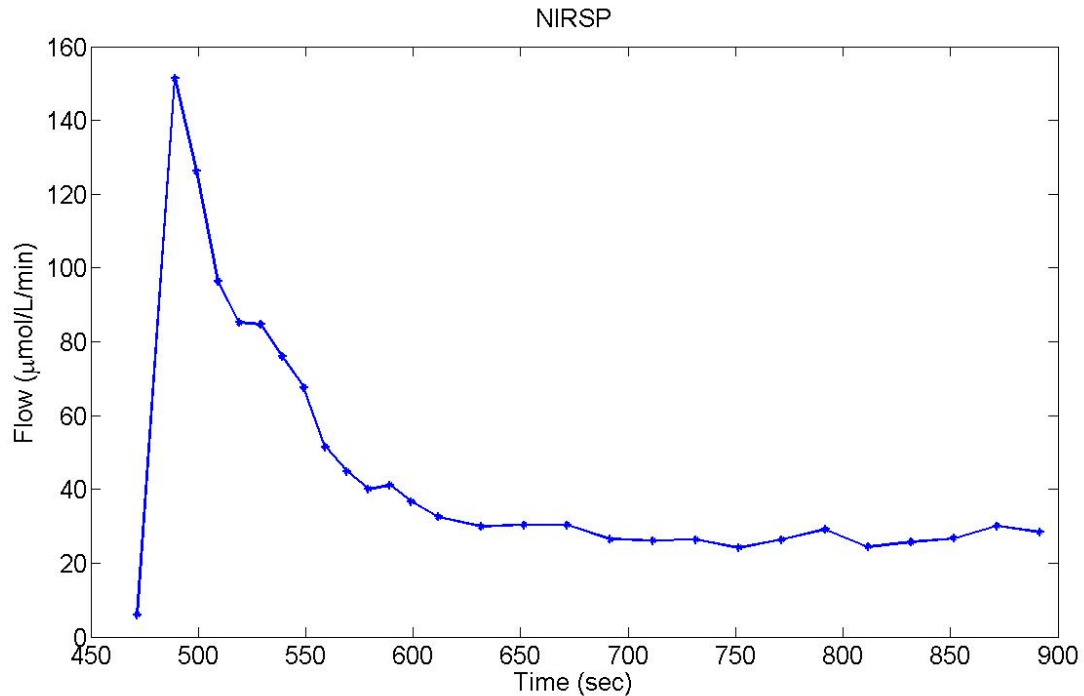


Figure 3-8: Blood flow variation during RH measured by NIRSP.

During ischemic period, the vascular impedance decreases markedly. This period is accompanied by a shortage of oxygen, arteries dilatation and a buildup of vasodilator metabolites. By releasing the arterial cuff, blood flow increases instantly and perfusion pressure is restored. The increase in blood flow washes the accumulated vasodilator metabolites away while inducing a remarkable amount of shear stress on vessel wall.

Sudden increase in vessel wall tension along with vasodilator metabolites washout, make the vascular muscle contract immediately after arterial cuff release. On the other hand, the sudden increase in blood flow elicits the release of endothelium derived dilator factors that may limit myogenic constriction thereby, reducing the enhanced level of shear stress on vessel walls. Consequently, tissue becomes re-oxygenated, vessels regain their normal vascular tone and blood flow returns to baseline (Figure 3-9). Therefore, the integrity of endothelial cells has an important effect on vascular tone retrieval.

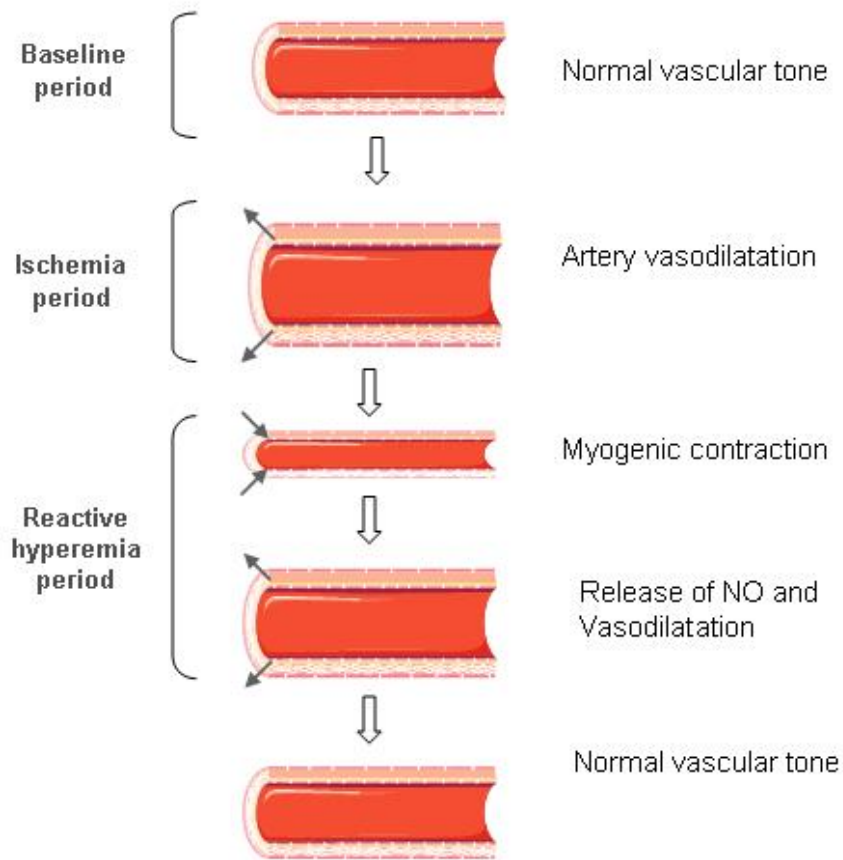


Figure 3-9: Vasoactivation steps during three stages of the experiment.

Blood flow measurements during the three steps of our protocol allowed following the variations in forearm vascular tone (Figure 3-10).

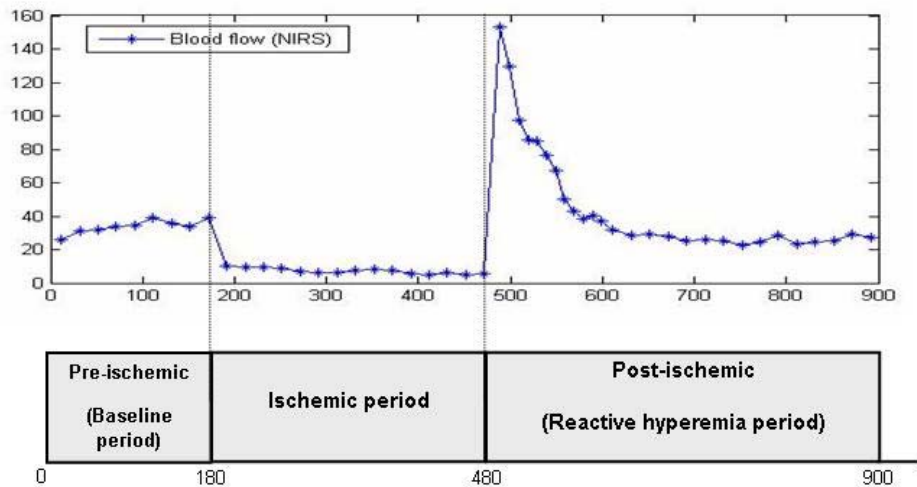


Figure 3-10: Blood flow measurement by NIRSP at three stages of study: pre-ischemic, ischemic and post-ischemic period.

The forearm blood flow plot during reactive hyperemia generally exhibited a bimodal form: the first peak occurred exactly after the release of arterial cuff while the second one arrived approximately 52 to 60 seconds later. The amplitude of the second one was smaller compared to the first one (Figure 3-8). We hypothesized that the peaks might be related to different mechanisms of endothelial dependent and independent vasoactivation. We attributed the first peak to myogenic response, which is endothelial independent, and the second one to endothelial dependent vasodilatation.

We based our assumptions on the fact that transition state at the release of ischemia is accompanied by sudden increase in blood flow and vascular pressure [14, 17, 18]. Increase in pressure elicits vascular muscles contraction that limits blood flow immediately; this event forms the first peak on blood flow plot during reactive hyperemia. Increase in blood flow at the onset of reactive hyperemia phase elicits the release of relaxing factors (NO) from endothelial cells [2, 12]. NO makes the vessels dilate and limits myogenic contraction. Maximal dilatation due to the release of NO occurs approximately one minute after arterial cuff deflation that forms the second peak [7, 26, 37].

Based on our hypothesis, we defined an index to quantify the capacity of vascular endothelial cells in releasing endogenous NO in comparison with the amount of stimuli on vessel wall. This factor could be compared among different subjects. We fitted a gamma variate function to each of the detected peaks during reactive hyperemia. We defined the following equation:

$$\eta_{factor} = \frac{AUC(Gamma_2)}{AUC(Gamma_1)} \quad (3.9)$$

where AUC represents the area under curve and $Gamma_1$ and $Gamma_2$ represent the first and second gamma variate functions respectively. The aim of this study is to verify the repeatability of the η_{factor} in the same subject after 3 and 24 hours. It has been established that most of the mechanical stress responses in endothelial cells disappear in 3 hours. However, there are still some effects such as cell surface stiffness and regulation of fibronectin synthesis, which remain up to 24 hours [15] (Table 1).

3.6.1 Subjects

After approval of the measurement protocol by the research and ethics committees of the Montreal Heart Institute, 15 healthy volunteers with low likelihood of CAD were recruited for the experiment (Table 3-2) [50].

Gender	6 men / 9 women	
Age	37 ± 10	
BMI	24.63 ± 5.55 kg/m ²	
Patients condition	Active smoker	n=1
	High blood pressure	n=2

Table 3-2: Patient population characteristics for experiment2.

3.6.2 Protocol

The protocol of the experience was the same as the previous study described in 3.2. We executed the same protocol three times on each subject, the second experiment was carried out 24 hours after the first one. The third experiment was performed 3 hours after the second one (27 hours

after the first experiment). In all three experiments, subjects were fasten to avoid probable effects of nutrients on vasodilatory mechanism of endothelial cells [52].

3.6.3 Setup

SGP and NIRS measurements were performed simultaneously with the same setup as the previous study described in 3.2. Studies began at 8:30 A.M. after a 12 hour fasting period. The experience was repeated twice the day after at 8:30 A.M., after a 12 hour fasting period, and at 11:30 after a 15 hour fasting period.

3.6.4 Data analysis

Gamma variate function fitting was based on a simplified formulation presented by Madsen et al [53]. They represent a function depending on four parameters among which there is no coupling. The gamma variate function with four independent parameters, y_{\max} , x_{\max} , x_0 and α is expressed as:

$$y = y_{\max} \left(\frac{x - x_0}{x_{\max} - x_0} \right)^{\alpha} \times e^{-\alpha \left(\frac{x - x_0}{x_{\max} - x_0} \right)} \quad (3.10)$$

A gamma variate function, with appropriate initial points was applied to the first part of the signal, including the first peak. Subtraction of the first gamma fit from the original blood flow curve yielded the second part, including the second peak. For a second time, a gamma variate function with appropriate initial points was fitted to the second part (Figure 3-11). We calculated the area under the curves for the two gamma functions and their ratio represented the η factor.

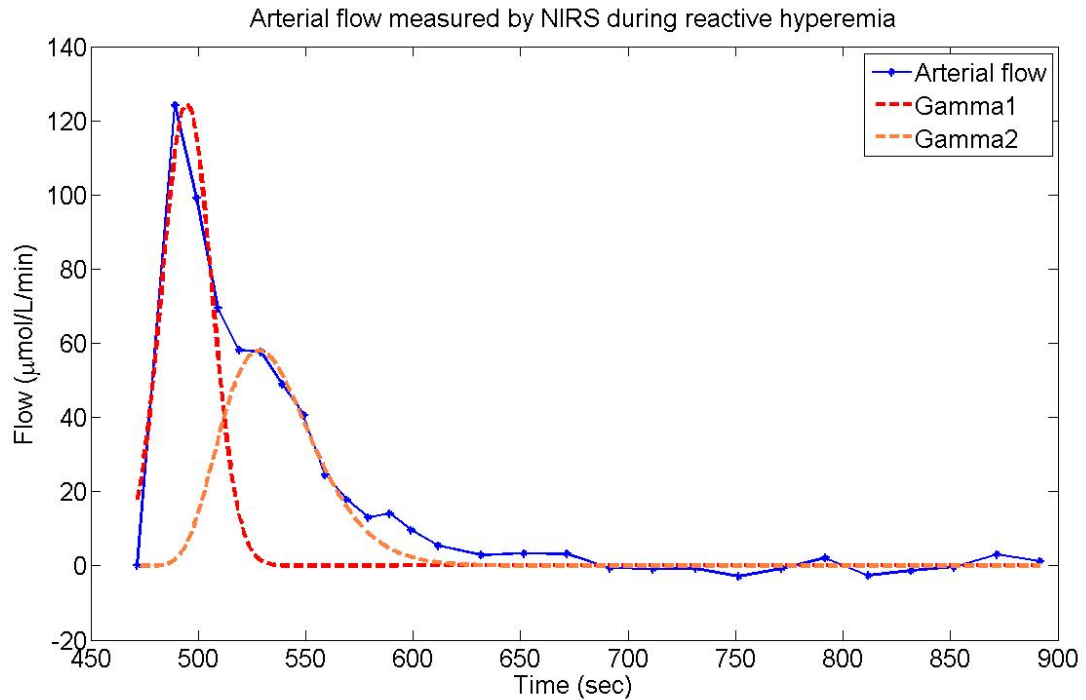


Figure 3-11: Gamma variate function fitting on the first and second detected peaks.

3.6.5 Statistical analysis

Statistical analysis was performed using the SPSS statistical package version 10.0 and GraphPad Prism version 5.01. We evaluated the repeatability of calculated η factor at 3h and 24h experiments through intra-class correlation coefficient. Linear regression was performed between the calculated η factors from the 3h and 24h experiments. We used repeated ANOVA test to verify the existence of a significant difference among the three repeated experiments. Statistical significance was accepted when the two-tailed p value was <0.05.

Chapter 4: Results

4.1 NIRS method vs. gold standard (SGP)

Repeatability

The repeatability of blood flow measurements at baseline for SGP and NIRSP were assessed using intra-class correlation coefficients (ICC). In this regard, nine resting baseline flow measurements were made at baseline. Left arm baseline blood flow was 3.36 ± 1.35 mL/100mL/min and 3.90 ± 1.74 mL/100mL/min for SGP and NIRS respectively ($p=0.10$).

During ischemic period, a decrease in blood flow was observed with both methods. By release of arterial occlusion, an acute increase in blood flow due to hyperemic reaction and flow restoration occurred. Blood flow remained increased for some minutes and returned approximately to normal when resistance vessels regained their normal vascular tone (Figure 4-1).

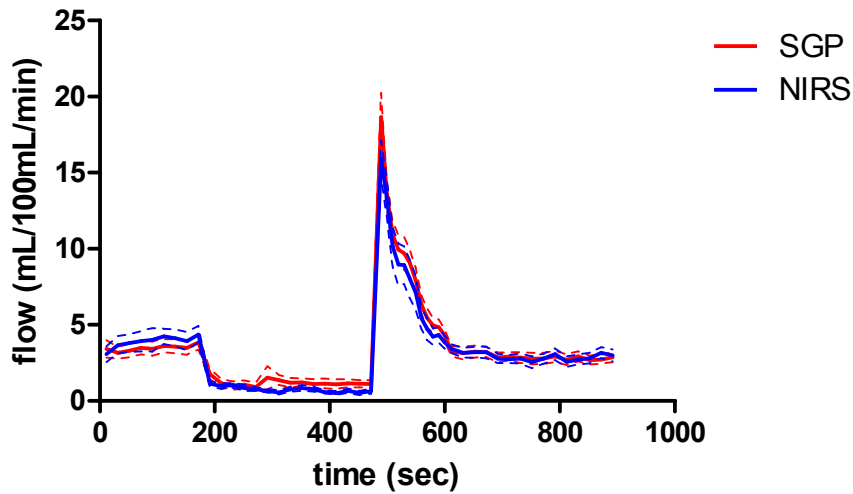


Figure 4-1: Left forearm blood flow measurements by NIRS and SGP during three stages of experience. Dashed lines represent the mean \pm standard error of the mean.

Both methods showed an excellent reproducibility at baseline with ICC of 0.98 (95% CI: 0.96 – 0.99; $p < 0.0001$) and 0.98 (95% CI: 0.95 – 0.99; $p < 0.0001$) for SGP and NIRS respectively.

Comparison of blood flow measurements during reactive hyperemia

Blood flow measurements during reactive hyperemia with both methods showed an excellent linear relationship with a correlation coefficient of 0.91 (95%, $p < 0.0001$) (Figure 4-2).

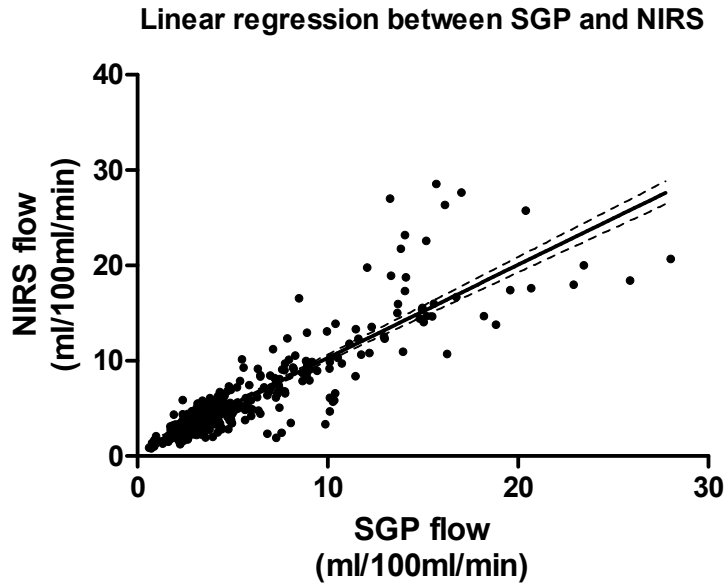


Figure 4-2: Linear regression between two modalities (SGP and NIRS).

A Bland-Altman plot allowed a better comparison between the two methods. As shown in Figure 4-3, NIRS tends to underestimate the high arterial inflows, at onset of reactive hyperemia stage. A linear regression between values of differences versus averages was performed. The slope was evaluated to be -0.1007 ± 0.02621 with a significant difference from zero.

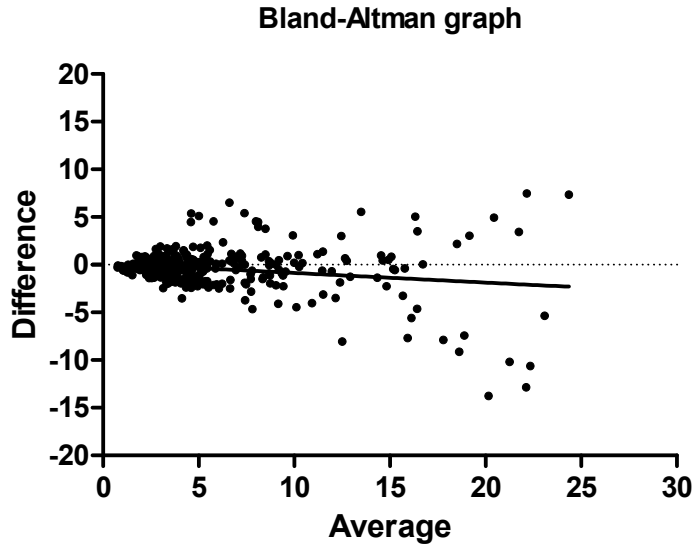


Figure 4-3: Bland-Altman graph of flow measurements with linear regression.

A two-way paired ANOVA test was performed to verify the effect of the two modalities on results during RH (Figure 4-4). Calculated F (0.33) is much smaller than critical threshold (2.44) indicating that there is no significant difference between flow measurement by the two modalities ($p = 0.5723$).

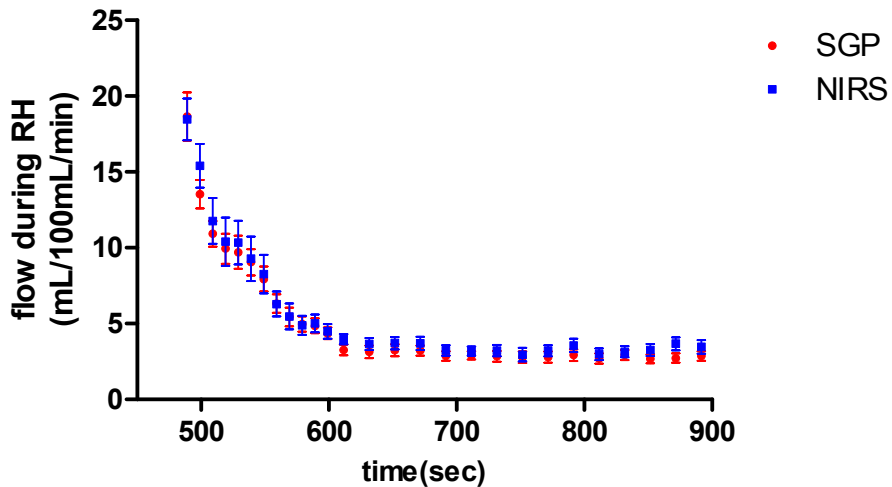


Figure 4-4: Blood flow measurements during RH by SGP and NIRS. Error bars represent standard error of the mean.

Comparison of blood flow measurements at baseline period and post-RH

In order to determine whether blood flow reaches the baseline level at the end of the experiment, we compared blood flow measurements at baseline and post-RH phases. We performed a paired student's *t*-test between repeated flow measurements at baseline and at the end of reactive hyperemia period (nine points). We observed a significant difference in flow measurements at post-RH stage compared to baseline for SGP ($p=0.0003$) and NIRS ($p=0.0030$) (Figure 4-5).

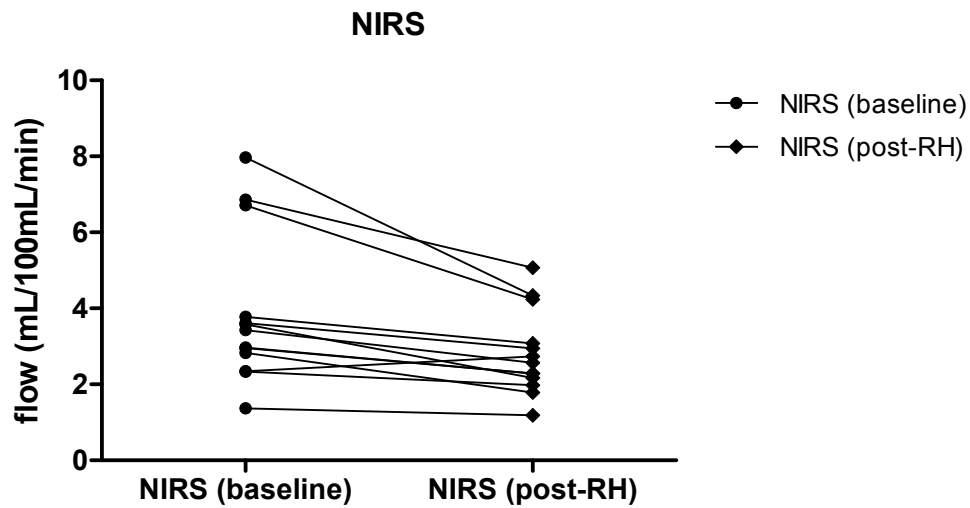


Figure 4-5: Comparison of flow measurements at baseline and post-RH period using paired student's *t*-test.

Blood flow measurement was performed on the right forearm by both the SGP and the NIRS methods to verify the probable influence of the left forearm reactive hyperemia. No significant variation in right forearm blood flow was observed during the three consecutive stages of the experiment.

4.2 η factor and repeatability

Measurements of η factor during three repeated experiments showed an excellent repeatability with ICC of 0.9313 (95%CI: 0.8368-0.9750).

A one-way ANOVA test revealed that there is no significant difference among the mean measurements of the three repeated experiments ($p=0.5779$) (Figure 4-6).

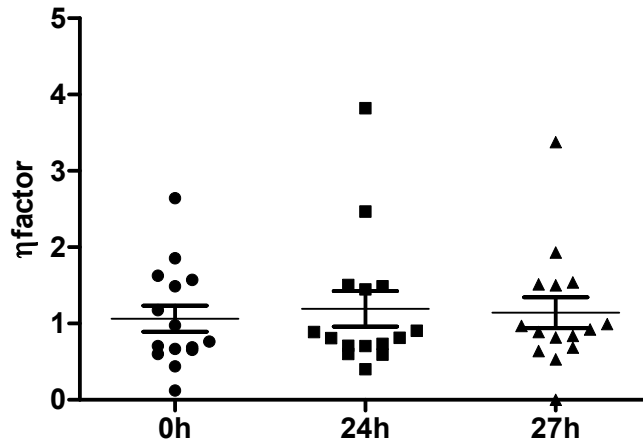


Figure 4-6: One-way ANOVA test showed that there is no significant difference among the three repeated groups of measurements.

Repeated η factor were highly concordant with the correlation coefficients of 0.8763 ($p < 0.0001$) and 0.8398 ($p < 0.0001$) for repeated measurements at 24h and 3h respectively (Figure 4-7 and 4-8).

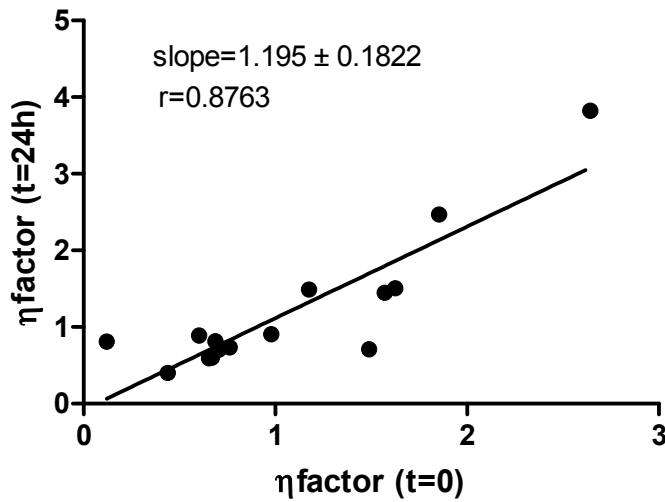


Figure 4-7: Linear regression between repeated measurements at $t=0$ and $t=24h$.

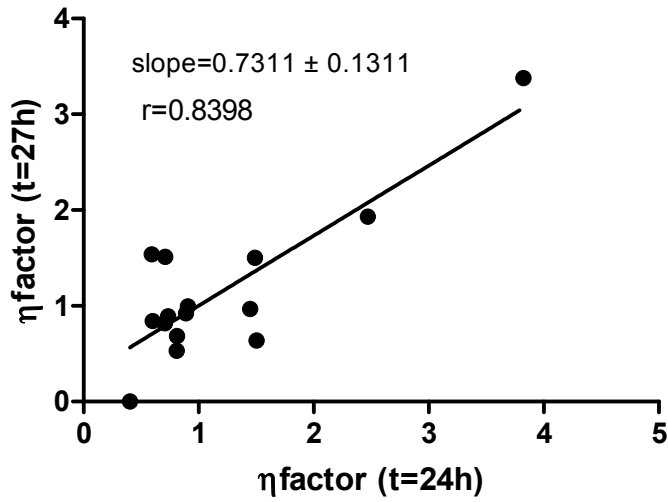


Figure 4-8: Linear regression between repeated measurements at t=24h and t=27h.

We calculated the time delay (in seconds) before the second detected peak (t_{peak}) occurs on the signal, based on the onset of the reactive hyperemia period. We obtained mean values of t_{peak} of: 59.11 sec. (95%CI: 52.95-65.25), 57.65 sec. (95%CI: 52.66-65.65) and 52.65 sec. (95%CI: 52.95-65.25) for experiments at t=0, t=24h and t=27h respectively. A one-way ANOVA test showed that there is no significant difference among the means of calculated t_{peak} at each experiment ($p=0.4813$) (Figure 4-9).

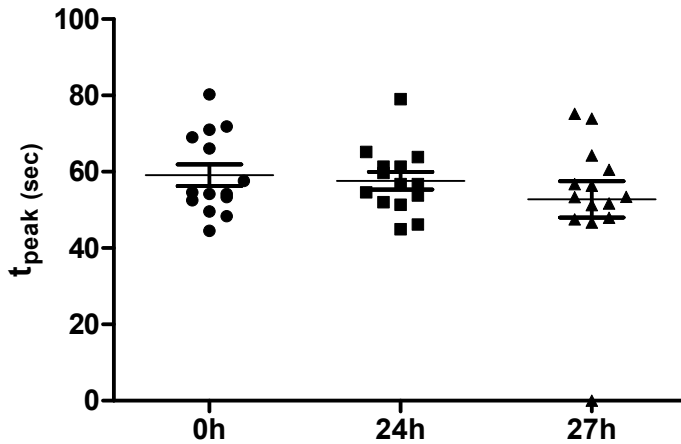


Figure 4-9: No significant difference was shown among the means t_{peak} at each experiment by one-way ANOVA test.

Chapter 5: Discussion

5.1 Oxygenation monitor NIRO-200

We showed that the measurement of the total hemoglobin variations during reactive hyperemia using an oxygenation monitor, Niro-200, is a good determinant of arterial inflow variations. We also performed flow measurements during reactive hyperemia by SGP and we presented data indicating that the NIRS technique yields values comparable to those obtained by SGP. Since the NIRS technique is currently used in clinic for cerebral and muscular tissue oxygenation monitoring, its application to other clinical tests such as reactive hyperemia and endothelial function might be of high interest. The Niro-200 tissular oximeter provides several parameters, which lead to measurements of blood volume variations during reactive hyperemia. We hypothesized that variations in total hemoglobin (oxygenated and deoxygenated) during consecutive venous occlusions are proportional to blood volume variations during these periods. The other advantage of Niro-200 compared to other clinical oxygenation monitor is the relatively high sampling rate (6 Hz), which is adequate for precisely calculating blood volume increase rate during venous occlusions (Figure 4-5). These characteristics, as well as its non-invasiveness may render this technology widespread in reactive hyperemia studies.

5.2 Forearm blood flow

In our study, we found a strong correlation between NIRS and SGP which is considered the gold standard. However, Bland-Altman plot showed that NIRS system tends to underestimate arterial inflow values at the onset of reactive hyperemia state while there is a sharp increase in blood flow (Figure 5-3). Many factors can explain lower flow values measured by NIRS. During the first two minutes of reactive hyperemia, we reduced venous occlusion times from 10 seconds to 5 seconds. This selection allowed us to obtain more blood flow values during this physiologically important period of time. However, shorter venous occlusion times may reduce the accuracy of upslope calculation as it does not provide sufficient time for venous outflow. In addition, the adipose tissue causes the near infrared light to disperse which in turn may decrease the amplitude of the NIRS signal particularly in overweight patients.

Despite the complete arterial occlusion (systolic pressure + 50 mmHg) during the ischemia period, increases in total hemoglobin during venous occlusion were still observed, which caused the detection of a small blood flow during this period (Figure 4-1). This increase in the amount of total hemoglobin was found in other studies and was attributed to arterial blood pooling into the venous reservoir of the forearm muscle during the ischemic period [33, 54].

The calculation of the blood volume increment rate during repeated venous occlusions yielded forearm blood flow values. Repetitive inflation and deflation of the venous cuff was accompanied with slight movements of the forearms throughout the experience. These movements affect the SGP signal by sharp rises at the onset of cuff inflation, which appears on the recorded signal (Figure 5-1). In order to avoid blood flow overestimation, we excluded the first part of the SGP signal from the upslope calculation. However, the NIRSP signal remained unaffected by the aforementioned movement artifact (Figure 5-1).

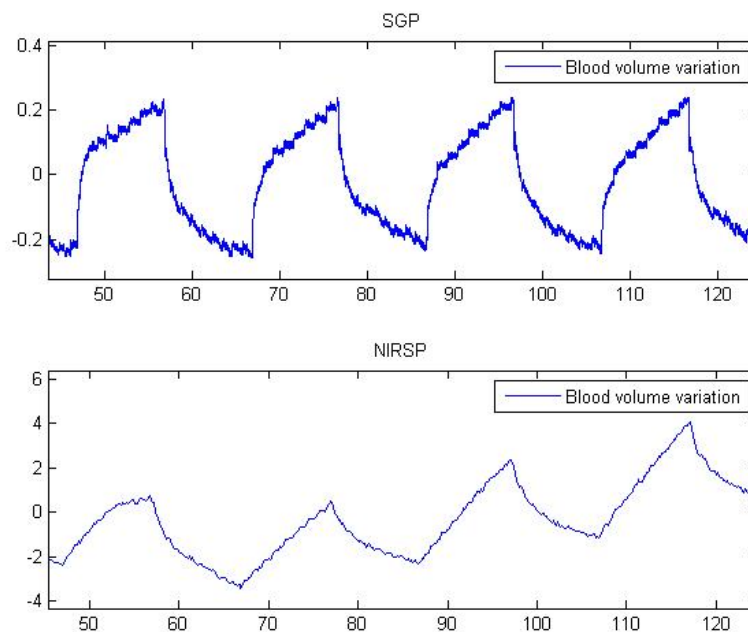


Figure 5-1: Blood volume variations during venous occlusions by SGP and NIRSP.

Baseline arterial inflow measurements obtained with both methods were similar to those reported by other studies [25, 55]. However, arterial inflow values measured by both methods at the end of experiment are significantly smaller as compared to the baseline (NIRSP: 2.822 ± 0.30 mL/100mL/min vs. 3.903 ± 0.30 mL/100mL/min). The equilibrium of vaso-active agents

produced by the endothelium is the main contributor to vascular tone regulation. The balance between vasodilator and vasoconstrictor agents is affected by reactive hyperemia, which seems to last for several hours [15]. We attributed the unsteadiness of the blood flow after reactive hyperemia to long-term changes in endothelial structure and morphology such as cell alignment along blood flow direction. The mentioned long-term changes in endothelial function and structure are due to an acute increase in the level of shear stress exerted on the endothelial cells which remains over a time period of more than 5 hours (Table 2-1) [15].

The forearm blood flow measured by the NIRS was expressed in $\mu\text{mol/L}/\text{min}$. Concentration changes of hemoglobin is provided in $\mu\text{mol/L}$ by the NIRS device. However, SGP is calibrated to provide blood flow variations in $\text{mL}/100\text{mL}/\text{min}$. The calculated blood flow variations by NIRS could be converted to $\text{mL}/100\text{mL}/\text{min}$ by individual hemoglobin concentration. The conversion could be performed by considering individual Hb concentration, the molecular weight of Hb and the molar ratio between Hb and O_2 (1:4). However, blood sampling is necessary to obtain individual Hb concentration. In order not to affect the non-invasive characteristic of our method, we converted blood flow units in $\mu\text{mol/L}/\text{min}$ to $\text{mL}/100\text{mL}/\text{min}$ using a universal calibration factor.

5.3 Other studies

A number of studies have been conducted on the assessment of endothelial function by the NIRS technique. But almost none of them had a similar methodology with which we could compare our results directly.

De Blasi et al. measured forearm blood flow by NIRS at rest and during the hyperemic response induced by hand exercise [56]. They performed three repetitive venous occlusions, each lasting 30 sec, during the reactive hyperemia to measure the blood volume changes. They presented the mean of the three measurements as the blood flow during reactive hyperemia. Nonetheless, they did not aim to obtain the blood flow variations over time.

We obtained 9 and 27 measures of blood flow during baseline and reactive hyperemia respectively. They found higher blood flow values measured by SGP compared to NIRS which is in agreement with our results. They found an increase in total hemoglobin variation during the ischemic period which is also in agreement with our results.

Kragelj et al. studied post occlusive hyperemic response using NIRS through an ischemic condition [33]. They monitored variations in oxy- and deoxy-hemoglobin during ischemia and hyperemic response. They calculated the time after the release of the cuff until the initial values of HbO₂ and the peak value in order to characterize endothelial function by variations in HbO₂. They found a significant difference in measured parameters among the subjects in spite of the fact that they were selected among healthy subjects. On our side, we defined a factor on blood flow variations during reactive hyperemia to test the endothelial function and three repeated measurements show a very good repeatability for the defined factor.

Edwards et al. described a methodology for blood flow measurement by NIRS [57]. The method is based on the Fick principle: flow could be quantified by relating the concentration of a tracer molecule in the vascular supply to the rate of tracer accumulation in the organ.

They considered the increase in arterial HbO₂ concentration as an intravascular tracer that is observable by NIRS. They applied a face mask to supply oxygen and nitrogen gases over the patient's face and nose in order to control the inspired oxygen concentration. In their methodology, a series of measurements were averaged and the mean value was presented as blood flow. They compared the results to those obtained with the SGP method and they found a strong correlation. However, their study was not designed to examine the reactive hyperemic response through blood flow measurements.

Some studies used methods other than post-ischemic reactive hyperemia, such as limb heating, to assess endothelial dependent vasodilatation. Local skin heating provides an increase in regional blood flow through a vasodilatation mechanism. However, the vasodilatory effect of heating is limited to the cutaneous layers and do not reach the muscular vascular bed [58]. On the other hand, it has been established that L-NMMA has no effect on flow mediated dilatation after hand warming, indicating that vasodilatation caused by limb warming is endothelial independent [27].

5.4 η factor and its clinical utility

Few studies have been conducted to assess the contribution and quantification of NO to post-ischemic reactive hyperemia in the human forearm. Meredith et al. studied forearm vasodilator responses in the absence and presence of NO synthesis inhibitor, L-NMMA, using the SGP method [59]. They defined the area under the flow-time curve at 1 and 5 min as hyperemic blood volumes. Their results indicated that in the presence of L-NMMA, the volume of blood at both 1

and 5 min reduced significantly. They demonstrated that NO contributes to post-ischemic vasodilatation. However, they did not characterize NO related and unrelated parts of the forearm blood flow during reactive hyperemia.

We attributed the second blood flow peak during reactive hyperemia to NO dependent vasodilatation. This peak occurs, on average, 55.08 (95%CI: 52.07-59.89) seconds after the release of the arterial cuff (Figure 5-9). This time delay is in agreement with other studies findings of the maximal post-ischemic vasodilatation instant due to NO release, through direct measurement of arterial diameter by Doppler ultrasound during reactive hyperemia [26]. However, the release of NO has never been detected by blood flow variations during reactive hyperemia.

We qualified the first peak as a sudden increase in blood flow due to the release of the arterial cuff, which was rapidly restricted by myogenic constriction. The first peak could represent the magnitude of the shear stress stimulus on the endothelial cells which trigger the release of NO. The amount of the released NO depends on the integrity of the endothelium as well as the magnitude of the stimulus [22]. Pyke et al. demonstrated that the shear rate stimulus varies between subjects while it remains constant within subjects [9]. Therefore, it is important to consider the amount of transferred stimulus to the endothelial cells, while interpreting the flow mediated vasodilatation response. We aimed to normalize the endothelium capacity in releasing relaxing factors according to the amount of shear stress by defining the *ηfactor*. A good level of repeatability was found within subjects for the calculated *ηfactor* (ICC=0.9313). We obtained mean *ηfactor* values of 1.065 (95%CI: 0.7009-1.430), 1.194 (95%CI: 0.6964-1.691) and 1.143 (95%CI: 0.7105-1.576) for repeated measurements at t=0, t=24h and t=27h respectively. However, there is no such quantification in other studies to compare the results with. Perhaps the most interesting aspect of our findings is having defined a reproducible parameter within subjects, which could be useful in the quantification of the endothelium capacity in releasing NO compared to the amount of deposited shear stress to endothelial cells.

As evaluation of endothelial function develops to become a practical mean in evaluation of patients at higher risk for cardiovascular events, it is important to question the clinical value of measuring the *ηfactor*. The *ηfactor* is a useful measure of NO dependent endothelial vasodilatation which may serve as an indication for cardiovascular risk factors. Atherosclerosis is present and clinically silent before the development of acute coronary events. At this point

cardiovascular disease risk factors are difficult to be screened because there is a time delay between the exposure to a risk factor and the cardiovascular disease manifestation. The *nfactor* may be considered as a strong predictive tool in patients with mild or high level risk factors. This prediction is achieved through quantification of NO contribution to the hyperemic response. Identification of those patients experiencing a reduced endothelial function can then be followed by definition of a subgroup including patients who would benefit from aggressive medical or lifestyle treatment. Treatment of risk factors in patients at high risk is associated with improved outcome. Furthermore, prevention of atherosclerosis at its early stage can have global health impact since it economizes several resources. There is currently no standard protocol for clinical application of the *nfactor*; repeated measures of the factor is required to avoid environmental factor effects such as ingestion of fatty foods and smoking which may lead to a false positive prognostic.

These potential utilities of the *nfactor* measurement will obviously need further studies before it is applied in clinical practices. Some of these studies are detailed in Chapter 6.

5.5 NIRS technique advantages and limitations

A variety of non-invasive techniques have been developed to study reactive hyperemia. Strain gauge plethysmography has been employed as the gold standard. This method, however, does not provide regional information since it detects variations of an undetermined part of the limb volume and the axial resolution is so poor with this technique. On the other hand, SGP is too sensitive to movement artifact which may limit its applicability in a clinical setting. Ultrasound Doppler is a useful tool for blood flow measurement in relatively large blood vessels but the technique is not sensitive to blood flow in smaller vessels. MRI and PET techniques could serve for blood flow measurement with high temporal and spatial resolutions [43, 44]. However, their clinical uses in studies of reactive hyperemia are limited due to high cost and poor mobility.

NIRS seems to be a promising alternative. It is not as sensitive to limb movement as SGP (Figure 6-1). It can provide information on oxygenation levels in relatively deep muscle tissue. Unlike ultrasound Doppler, it is sensitive to small vessels such as arterioles and venules. Unlike MRI and PET, NIRS provides low spatial resolution but it provides relatively high temporal resolution while being inexpensive and mobile.

The NIRS monitors oxygenation levels in muscle tissue and resistive vessels such as arterioles, capillaries and venules. However, large vessels such as conductance vessels are out of scope for NIRS due to vessel wall thickness.

Myoglobin has identical absorption spectra to hemoglobin and the two species are not separable by actual NIRS systems. However, in resting muscle with relatively low metabolism rate, myoglobin accounts for less than 10% of the total NIRS signal and its contribution to the signal remains constant [57]. In our study, we assumed that myoglobin saturation is constant during the experiment.

The NIRS signal is a combination of three light absorbencies: hemoglobin in arterial space, hemoglobin in venous space and myoglobin in muscle. Therefore, the NIRS system is not able to distinguish arterial and venous flow. In our technique, however, we repeatedly cut the venous outflow to measure the arterial inflow specifically.

One of the principle drawbacks of the NIRS method may be the qualitative nature of its measurements. The pathlength of NIR light in tissue is unknown for continuous light. Therefore, the light absorption level monitored by NIRS device does not provide absolute levels of oxy- and deoxy-hemoglobin concentration. The NIRS measurements are provided in variations compared with a zero point that is set at the beginning of each experiment.

Skin and subcutaneous fat contribute a slight amount to oxygen saturation. Since adipose tissue thickness might be different between genders, additional care should be taken concerning this issue.

This problem increases in patients with relatively thick fat layer and it would decrease the signal to noise ratio of the NIRS signal; this fact may limit the applicability of NIRS for overweight patients. Standardization of the NIRS setup in blood flow measurement is an important issue since the displacement of the NIRS probes has a remarkable effect on the amplitude of the signal.

Chapter 6: Conclusion

We assessed the efficiency of using NIRS to evaluate changes in vascular tone during reactive hyperemia. To characterize blood flow variations during this period through endothelial dependent and independent responses, two experiments were designed. The results of the first experiment showed a strong correlation between measurement of the blood flow by NIRS and SGP. This study indicated that measurement of forearm arterial inflow is possible in a precise and totally non-invasive way through NIRS. The results could be used to obtain valuable new information about the integrity of peripheral vascular endothelium in releasing vasodilator agents. Therefore, in the second experiment, we presented a repeatable factor which was mainly defined to reveal endothelium capacity in releasing of vasodilator agents. The proposed factor could be served as determinant of NO contribution to hyperemic response. This new factor might be useful in better understanding the endothelial function in patients with atherosclerotic risk factors. This was the first series of studies to investigate the possibility of endothelial function quantification through measurements of forearm blood flow.

Future research to validate the capacity of η factor in endothelial function quantification is proposed as:

- 1) Assessment of the η factor obtained through NIRS with other non-invasive techniques of blood flow measurement such as Ultrasound Doppler; this study could lead to the examination of the reproducibility of η factor by other established techniques of blood flow measurements.
- 2) Evaluation of the η factor obtained in presence and absence of NO synthesis inhibitors; this study could lead to quantify the contribution of endothelium-derived NO to post-ischemic reactive hyperemia response.
- 3) Comparison of the η factor obtained in a group of patient with atherosclerotic diseases with ones obtained in a group of control; this study investigates the ability of the η factor in differentiating the group of patients from the control group. Significant results would lead to determine a threshold for impaired reactive hyperemic responses.

Bibliography:

- [1] N. Weiss, C. Keller, U. Hoffmann, and J. Loscalzo, "Endothelial dysfunction and atherothrombosis in mild hyperhomocysteinemia," *Vasc Med*, vol. 7, pp. 227-39, 2002.
- [2] G. H. Gibbons and V. J. Dzau, "The emerging concept of vascular remodeling," *N Engl J Med*, vol. 330, pp. 1431-8, 1994.
- [3] A. Balbatun, F. R. Louka, and T. Malinski, "Dynamics of nitric oxide release in the cardiovascular system," *Acta Biochim Pol*, vol. 50, pp. 61-8, 2003.
- [4] F. A. Jane A. Mitchell, Lucy Bailey, Laura Moreno and Louise S. Harrington, "Role of nitric oxide and prostacyclin as vasoactive hormones released by the endothelium " *Experimental Physiology*, vol. 93, pp. 141-147, 2007.
- [5] A. Vertes and A. Kali, "[Endothelium-dependent and independent vasodilation in young males with previous myocardial infarction]," *Orv Hetil*, vol. 144, pp. 1025-9, 2003.
- [6] U. Forstermann, A. Mugge, U. Alheid, A. Haverich, and J. C. Frolich, "Selective attenuation of endothelium-mediated vasodilation in atherosclerotic human coronary arteries," *Circ Res*, vol. 62, pp. 185-90, 1988.
- [7] T. J. Anderson, A. Uehata, M. D. Gerhard, I. T. Meredith, S. Knab, D. Delagrang, E. H. Lieberman, P. Ganz, M. A. Creager, A. C. Yeung, and et al., "Close relation of endothelial function in the human coronary and peripheral circulations," *J Am Coll Cardiol*, vol. 26, pp. 1235-41, 1995.
- [8] N. Benjamin, A. Calver, J. Collier, B. Robinson, P. Vallance, and D. Webb, "Measuring forearm blood flow and interpreting the responses to drugs and mediators," *Hypertension*, vol. 25, pp. 918-23, 1995.
- [9] K. E. Pyke, E. M. Dwyer, and M. E. Tschakovsky, "Impact of controlling shear rate on flow-mediated dilation responses in the brachial artery of humans," *J Appl Physiol*, vol. 97, pp. 499-508, 2004.
- [10] O. Traub and B. C. Berk, "Laminar shear stress: mechanisms by which endothelial cells transduce an atheroprotective force," *Arterioscler Thromb Vasc Biol*, vol. 18, pp. 677-85, 1998.
- [11] K. E. Pyke and M. E. Tschakovsky, "The relationship between shear stress and flow-mediated dilatation: implications for the assessment of endothelial function," *J Physiol*, vol. 568, pp. 357-69, 2005.
- [12] M. Ohno, G. H. Gibbons, V. J. Dzau, and J. P. Cooke, "Shear stress elevates endothelial cGMP. Role of a potassium channel and G protein coupling," *Circulation*, vol. 88, pp. 193-7, 1993.
- [13] R. Busse, G. Edwards, M. Feletou, I. Fleming, P. M. Vanhoutte, and A. H. Weston, "EDHF: bringing the concepts together," *Trends Pharmacol Sci*, vol. 23, pp. 374-80, 2002.
- [14] R. Schubert and M. J. Mulvany, "The myogenic response: established facts and attractive hypotheses," *Clin Sci (Lond)*, vol. 96, pp. 313-26, 1999.
- [15] G. K. John A. Bevan, Gabor M. Rubanyi, "Flow-Dependent Regulation of Vascular Function," 1995
- [16] N. Gokce, J. F. Keaney, Jr., L. M. Hunter, M. T. Watkins, J. O. Menzoian, and J. A. Vita, "Risk stratification for postoperative cardiovascular events via noninvasive assessment of endothelial function: a prospective study," *Circulation*, vol. 105, pp. 1567-72, 2002.

- [17] P. Coats, F. Johnston, J. MacDonald, J. J. McMurray, and C. Hillier, "Signalling mechanisms underlying the myogenic response in human subcutaneous resistance arteries," *Cardiovasc Res*, vol. 49, pp. 828-37, 2001.
- [18] G. A. Meininger, D. C. Zawieja, J. C. Falcone, M. A. Hill, and J. P. Davey, "Calcium measurement in isolated arterioles during myogenic and agonist stimulation," *Am J Physiol*, vol. 261, pp. H950-9, 1991.
- [19] M. L. Hijmering, E. S. Stroes, J. Olijhoek, B. A. Hutten, P. J. Blankestijn, and T. J. Rabelink, "Sympathetic activation markedly reduces endothelium-dependent, flow-mediated vasodilation," *J Am Coll Cardiol*, vol. 39, pp. 683-8, 2002.
- [20] P. C. Johnson, "Clinical methods for the evaluation of endothelial function-- a focus on resistance arteries
" *J Hypertens Suppl*, vol. 7, pp. S33-9; discussion S40, 1989.
- [21] M. C. Gonzalez, S. M. Arribas, F. Molero, and M. S. Fernandez-Alfonso, "Effect of removal of adventitia on vascular smooth muscle contraction and relaxation," *Am J Physiol Heart Circ Physiol*, vol. 280, pp. H2876-81, 2001.
- [22] G. F. Mitchell, H. Parise, J. A. Vita, M. G. Larson, E. Warner, J. F. Keaney, Jr., M. J. Keyes, D. Levy, R. S. Vasan, and E. J. Benjamin, "Local shear stress and brachial artery flow-mediated dilation: the Framingham Heart Study," *Hypertension*, vol. 44, pp. 134-9, 2004.
- [23] A. M. Malek, S. L. Alper, and S. Izumo, "Hemodynamic shear stress and its role in atherosclerosis," *Jama*, vol. 282, pp. 2035-42, 1999.
- [24] D. N. Ku, D. P. Giddens, C. K. Zarins, and S. Glagov, "Pulsatile flow and atherosclerosis in the human carotid bifurcation. Positive correlation between plaque location and low oscillating shear stress," *Arteriosclerosis*, vol. 5, pp. 293-302, 1985.
- [25] Y. Ishibashi, N. Takahashi, T. Shimada, T. Sugamori, T. Sakane, T. Umeno, Y. Hirano, N. Oyake, and Y. Murakami, "Short duration of reactive hyperemia in the forearm of subjects with multiple cardiovascular risk factors," *Circ J*, vol. 70, pp. 115-23, 2006.
- [26] P. Leeson, S. Thorne, A. Donald, M. Mullen, P. Clarkson, and J. Deanfield, "Non-invasive measurement of endothelial function: effect on brachial artery dilatation of graded endothelial dependent and independent stimuli," *Heart*, vol. 78, pp. 22-7, 1997.
- [27] M. J. Mullen, R. K. Kharbanda, J. Cross, A. E. Donald, M. Taylor, P. Vallance, J. E. Deanfield, and R. J. MacAllister, "Heterogenous nature of flow-mediated dilatation in human conduit arteries in vivo: relevance to endothelial dysfunction in hypercholesterolemia," *Circ Res*, vol. 88, pp. 145-51, 2001.
- [28] I. Eskurza, D. R. Seals, C. A. DeSouza, and H. Tanaka, "Pharmacologic versus flow-mediated assessments of peripheral vascular endothelial vasodilatory function in humans," *Am J Cardiol*, vol. 88, pp. 1067-9, 2001.
- [29] V. Schachinger and A. M. Zeiher, "Atherosclerosis-associated endothelial dysfunction," *Z Kardiol*, vol. 89 Suppl 9, pp. IX/70-4, 2000.
- [30] B. L. Langille, J. J. Graham, D. Kim, and A. I. Gotlieb, "Dynamics of shear-induced redistribution of F-actin in endothelial cells in vivo," *Arterioscler Thromb*, vol. 11, pp. 1814-20, 1991.
- [31] M. Uematsu, A. Kitabatake, J. Tanouchi, Y. Doi, T. Masuyama, K. Fujii, Y. Yoshida, H. Ito, K. Ishihara, M. Hori, and et al., "Reduction of endothelial microfilament bundles in the low-shear region of the canine aorta. Association with intimal plaque formation in hypercholesterolemia," *Arterioscler Thromb*, vol. 11, pp. 107-15, 1991.

- [32] Y. Yamashita, A. Maki, and H. Koizumi, "Wavelength dependence of the precision of noninvasive optical measurement of oxy-, deoxy-, and total-hemoglobin concentration," *Med Phys*, vol. 28, pp. 1108-14, 2001.
- [33] R. Kragelj, T. Jarm, and D. Miklavcic, "Reproducibility of parameters of postocclusive reactive hyperemia measured by near infrared spectroscopy and transcutaneous oximetry," *Ann Biomed Eng*, vol. 28, pp. 168-73, 2000.
- [34] H. Koizumi, T. Yamamoto, A. Maki, Y. Yamashita, H. Sato, H. Kawaguchi, and N. Ichikawa, "Optical topography: practical problems and new applications," *Appl Opt*, vol. 42, pp. 3054-62, 2003.
- [35] C.-W. S. Cheng-Kuang Lee¹, Po-Lei Lee³, Hsiang-Chieh Lee¹, C. C. Yang¹, Cho- and Y.-P. T. Pei Jiang², Tzu-Chen Yeh⁴, and Jen-Chuen Hsieh⁴, "Study of photon migration with various source detector separations in near-infrared spectroscopic brain imaging based on threedimensional Monte Carlo modeling," *Optics Express*, vol. 13, pp. 8339-8348, 2005.
- [36] G. Yu, T. Durduran, G. Lech, C. Zhou, B. Chance, E. R. Mohler, 3rd, and A. G. Yodh, "Time-dependent blood flow and oxygenation in human skeletal muscles measured with noninvasive near-infrared diffuse optical spectroscopies," *J Biomed Opt*, vol. 10, pp. 024027, 2005.
- [37] R. Wariar, J. N. Gaffke, R. G. Haller, and L. A. Bertocci, "A modular NIRS system for clinical measurement of impaired skeletal muscle oxygenation," *J Appl Physiol*, vol. 88, pp. 315-25, 2000.
- [38] H. S. Brown, M. Halliwell, M. Qamar, A. E. Read, J. M. Evans, and P. N. Wells, "Measurement of normal portal venous blood flow by Doppler ultrasound," *Gut*, vol. 30, pp. 503-9, 1989.
- [39] J. R. Libonati, M. Cox, N. Incanno, S. K. Melville, F. C. Musante, H. L. Glassberg, and M. Guazzi, "Brief periods of occlusion and reperfusion increase skeletal muscle force output in humans," *Cardiologia*, vol. 43, pp. 1355-60, 1998.
- [40] G. E. Nilsson, T. Tenland, and P. A. Oberg, "Evaluation of a laser Doppler flowmeter for measurement of tissue blood flow," *IEEE Trans Biomed Eng*, vol. 27, pp. 597-604, 1980.
- [41] C. Binggeli, L. E. Spieker, R. Corti, I. Sudano, V. Stojanovic, D. Hayoz, T. F. Luscher, and G. Noll, "Statins enhance postischemic hyperemia in the skin circulation of hypercholesterolemic patients: a monitoring test of endothelial dysfunction for clinical practice?," *J Am Coll Cardiol*, vol. 42, pp. 71-7, 2003.
- [42] P. C. van Zijl, S. M. Eleff, J. A. Ulatowski, J. M. Oja, A. M. Ulug, R. J. Traystman, and R. A. Kauppinen, "Quantitative assessment of blood flow, blood volume and blood oxygenation effects in functional magnetic resonance imaging," *Nat Med*, vol. 4, pp. 159-67, 1998.
- [43] R. S. Richardson, E. A. Noyszewski, L. J. Haseler, S. Bluml, and L. R. Frank, "Evolving techniques for the investigation of muscle bioenergetics and oxygenation," *Biochem Soc Trans*, vol. 30, pp. 232-7, 2002.
- [44] W. Burchert, S. Schellong, J. van den Hoff, G. J. Meyer, K. Alexander, and H. Hundeshagen, "Oxygen-15-water PET assessment of muscular blood flow in peripheral vascular disease," *J Nucl Med*, vol. 38, pp. 93-8, 1997.
- [45] F. Harel, J. Dupuis, A. Benelfassi, N. Ruel, and J. Gregoire, "Radionuclide plethysmography for noninvasive evaluation of peripheral arterial blood flow," *Am J Physiol Heart Circ Physiol*, vol. 289, pp. H258-62, 2005.

- [46] F. Harel, Q. Ngo, V. Finnerty, E. Hernandez, P. Khairy, and J. Dupuis, "Mobile detection system to evaluate reactive hyperemia using radionuclide plethysmography," *Physiol Meas*, vol. 28, pp. 953-62, 2007.
- [47] M. C. Conrad and H. D. Green, "Evaluation of venous occlusion plethysmograph," *J Appl Physiol*, vol. 16, pp. 289-92, 1961.
- [48] K. L. Berry, R. A. Skyrme-Jones, and I. T. Meredith, "Occlusion cuff position is an important determinant of the time course and magnitude of human brachial artery flow-mediated dilation," *Clin Sci (Lond)*, vol. 99, pp. 261-7, 2000.
- [49] S. N. Doshi, K. K. Naka, N. Payne, C. J. Jones, M. Ashton, M. J. Lewis, and J. Goodfellow, "Flow-mediated dilatation following wrist and upper arm occlusion in humans: the contribution of nitric oxide," *Clin Sci (Lond)*, vol. 101, pp. 629-35, 2001.
- [50] G. A. Diamond and J. S. Forrester, "Analysis of probability as an aid in the clinical diagnosis of coronary-artery disease," *N Engl J Med*, vol. 300, pp. 1350-8, 1979.
- [51] F. Harel, N. Olamaei, Q. Ngo, J. Dupuis, and P. Khairy, "Arterial flow measurements during reactive hyperemia using NIRS," *Physiol Meas*, vol. 29, pp. 1033-40, 2008.
- [52] C. Giannattasio, A. Zoppo, G. Gentile, M. Failla, A. Capra, F. M. Maggi, A. Catapano, and G. Mancina, "Acute effect of high-fat meal on endothelial function in moderately dyslipidemic subjects," *Arterioscler Thromb Vasc Biol*, vol. 25, pp. 406-10, 2005.
- [53] M. T. Madsen, "A simplified formulation of the gamma variate function," *Phys. Med. Bid.*, vol. 37, pp. 1597-1600, 1992.
- [54] T. R. Cheatle, L. A. Potter, M. Cope, D. T. Delpy, P. D. Coleridge Smith, and J. H. Scurr, "Near-infrared spectroscopy in peripheral vascular disease," *Br J Surg*, vol. 78, pp. 405-8, 1991.
- [55] A. C. Betik, V. B. Luckham, and R. L. Hughson, "Flow-mediated dilation in human brachial artery after different circulatory occlusion conditions," *Am J Physiol Heart Circ Physiol*, vol. 286, pp. H442-8, 2004.
- [56] R. A. De Blasi, M. Ferrari, A. Natali, G. Conti, A. Mega, and A. Gasparetto, "Noninvasive measurement of forearm blood flow and oxygen consumption by near-infrared spectroscopy," *J Appl Physiol*, vol. 76, pp. 1388-93, 1994.
- [57] A. D. Edwards, C. Richardson, P. van der Zee, C. Elwell, J. S. Wyatt, M. Cope, D. T. Delpy, and E. O. Reynolds, "Measurement of hemoglobin flow and blood flow by near-infrared spectroscopy," *J Appl Physiol*, vol. 75, pp. 1884-9, 1993.
- [58] R. Joannides, A. Costentin, M. Iacob, P. Compagnon, A. Lahary, and C. Thuillez, "Influence of vascular dimension on gender difference in flow-dependent dilatation of peripheral conduit arteries," *Am J Physiol Heart Circ Physiol*, vol. 282, pp. H1262-9, 2002.
- [59] I. T. Meredith, K. E. Currie, T. J. Anderson, M. A. Roddy, P. Ganz, and M. A. Creager, "Postischemic vasodilation in human forearm is dependent on endothelium-derived nitric oxide," *Am J Physiol*, vol. 270, pp. H1435-40, 1996.